Non-technical Summary

Lidar Altimeter Measurements of Canopy Structure:
Methods and Validation for Closed-Canopy, Broadleaf Forests
D.J. Harding, M.A. Lefsky, G.G. Parker, and J.B. Blair

For submission to Remote Sensing of Environment

The spatial organization of the vegetation components making up a forest canopies, including needles, leaves, branches and stems, has important connections to the way forests function as ecosystems. Examples of those connections are the dependence of: 1) the quality of animal and plant habitat on the volume and heterogeneity of living space within forest stands, 2) microclimate conditions like temperature and humidity on stand closure and the size and frequency of gaps within the forest, 3) the balance of energy, carbon dioxide and water vapor fluxes with the lower atmosphere on the topography of the outer canopy and total canopy surface area. Characterization of canopy structure is difficult to accomplish on the ground, being laborious and limited in extent, and is a major challenge for traditional remote sensing techniques, particularly for forests with moderate to high biomass. We evaluate the capabilities of lidar altimetry, a remote sensing technique recently developed at Goddard Space Flight Center, to quantitatively characterize the vertical structure of closed-canopy, broadleaf forests such as those typical of the deciduous forests of the eastern United States. Lidar, an acronym which stands for Light Detection and Ranging, utilizes a transmitted laser pulse and records the intensity of laser energy reflected back from a target as a function of time. In this study methods are developed to derive the vertical density of plant surface area from the laser energy reflected from the canopy surfaces and underlying ground. Lidar altimetry data was acquired by an airborne instrument referred to as SLICER (Scanning Lidar Imager of Canopies by Echo Recovery) for four stands in eastern Maryland. The stands are representative of typical forests in an age sequence from very young to old-growth and exhibit a large variation in vertical structure. Observations of canopy vertical structure collected from the ground are compared to the SLICER results. Good agreement between the two approaches indicates that they are each providing an accurate depiction of canopy structure. Unlike the limited ground observations, however, the SLICER data can be used to construct profiles through the forest stands at 10 m horizontal resolution that portray the vertical density of vegetation. The profiles reveal important spatial variations in vertical structure, such as the height and roughness of the canopy top and the location and extent of canopy stories and gaps. This new measurement capability will be implemented on a global basis by the Vegetation Canopy Lidar mission, scheduled for launch in 2000.

IN REVIEW, Remote Sensing of Environment

Lidar Altimeter Measurements of Canopy Structure: Methods and Validation for Closed-Canopy, Broadleaf Forests

D.J. Harding[1], M.A. Lefsky[2], G.G. Parker[3], and J.B. Blair[1]

[1] Laboratory for Terrestrial Physics, NASA Goddard Space Flight Center, Greenbelt, MD 20771, harding@denali.gsfc.nasa.gov, bryan@eib1.gsfc.nasa.gov

[2] USDA Forest Service, Forest Sciences Laboratory, Pacific Northwest Research Station, Corvalis, OR 97331, lefsky@fsl.orst.edu

[3] Smithsonian Environmental Research Center, P.O. Box 28, Edgewater, MD 21037, parker@serc.si.edu

Running head: Lidar Altimeter Measurements of Canopy Structure

Figures: 10

Tables: 7

Galley and proof correspondence to:
David J. Harding
Mail Code 921
NASA Goddard Space Flight Center
Greenbelt, MD 20771
Telephone: 301-614-6503
Fax: 301-614-6522
Email: harding@denali.gsfc.nasa.gov

1.0 ABSTRACT

Lidar altimeter observations of vegetated landscapes provide a time-resolved measure of laser pulse backscatter energy from canopy surfaces and the underlying ground. Airborne lidar altimeter data was acquired using the Scanning Lidar Imager of Canopies by Echo Recovery (SLICER) for a successional sequence of four, closed-canopy, deciduous forest stands in eastern Maryland. The four stands were selected so as to include a range of canopy structures of importance to forest ecosystem function, including variation in the height and roughness of the outer-most canopy surface and the vertical organization of canopy stories and gaps. The character of the SLICER backscatter signal is described and a method is developed that accounts for occlusion of the laser energy by canopy surfaces, transforming the backscatter signal to a canopy height profile (CHP) that quantitatively represents the relative vertical distribution of canopy surface area. The transformation applies an increased weighting to the backscatter amplitude as a function of closure through the canopy and assumes a horizontally random distribution of the canopy components. SLICER CHPs, averaged over areas of overlap where lidar ground tracks interesect, are shown to be highly reproducible. CHP transects across the four stands reveal spatial variations in vegetation, at the scale of the individual 10 m diameter laser footprints, within and between stands. Averaged SLICER CHPs are compared to analogous height profile results derived from ground-based sightings to plant intercepts measured on plots within the four stands. The plots were located on the segments of the lidar ground tracks from which averaged SLICER CHPs were derived, and the ground observations were acquired within two weeks of the SLICER data acquisition to minimize temporal change. The differences in canopy structure between the four stands is similarly described by the SLICER and ground-based CHP results, however a Chi-square test of similarity documents differences that are statistically significant. The differences are discussed in terms of measurement properties that define the smoothness of the resulting CHPs and

canopy properties that may vertically bias the CHP representations of canopy structure. The statistical differences are most likely due to the more noisy character of the ground-based CHPs, especially high in the canopy where ground-based sightings are rare resulting in an underestimate of canopy surface area and height, and to departures from the assumption of horizontal randomness which bias the CHPs toward the observer (upward for SLICER and downward for ground-based CHPs). The results demonstrate that the SLICER observations reliably provide a measure of canopy structure that reveals ecologically interesting structural variations such as those characterizing a successional sequence of closed-canopy, broadleaf forest stands.

2.0 INTRODUCTION

Characterization of canopy structure is a major challenge in remote sensing, particularly for moderate to high biomass forests. Remote sensing approaches to measuring canopy structure (reviewed in Weishampel et al., 1996) depend strongly on the electromagnetic wavelength used and the sensor's spatial resolution. Passive, visible to mid-infrared optical sensors rely on solar illumination reflected mostly from the outer canopy surface. The intensity of the reflected signal is dependent on numerous, intermixed factors some of which relate to structure (i.e., composition, geometry and density of canopy components) and some of which are unrelated (background composition, solar illumination and sensor view angles, and atmospheric transmittance). These sensors have been found to be insensitive to changes in biophysical parameters for moderately high to high-biomass systems. The problem is perhaps best exemplified by the abundant research on remote sensing of leaf area index (LAI) and biomass. Numerous publications reveal the limitations of passive optical images in estimating these variables, with useful results applying only to the lower half of the range over which these parameters vary (e.g., Sader and Joyce, 1990; Spanner et al., 1990; Lathrop and Pierce, 1991; Nemani et al., 1993; Chen and Cihlar, 1996).

The longer wavelengths used by active synthetic aperture radar (SAR) polarimetry systems enable remote sampling of structure throughout a greater depth of vegetation canopies (Ulaby et al., 1986). The intensity and polarization of the reflected radar signal are related to structural attributes of the canopy, but are a function of complex, wavelength-dependent scattering interactions with foliage, branches, trunks and the ground (e.g., Sun and Ranson, 1995). In addition, like passive optical systems, radar polarimetry is insensitive to biophysical parameters at moderate to high-biomass levels (e.g., Le Toan et al., 1992;

Dobson et al., 1995; Ranson et al., 1997; Imhoff, 1995). Active SAR interferometry offers a potentially powerful new method to remotely characterize canopy height characteristics. Whereas SAR polarimetry is primarily sensitive to the shape and orientation of canopy components, SAR interferometry is primarily sensitive to the spatial distribution of radar scattering elements within the canopy (Treuhaft and Moghaddam, 1998). However, interferometry methods to date have depended on assumptions about, or independent knowledge of, canopy structure and/or ground topography in order to derive vegetation height information from the interferometric phase data (Hagberg et al., 1995; Treuhaft et al., 1996; Askne et al., 1997; Cloude and Papthanassiou, 1998; Dammert and Askne, 1998; Rodriguez et al., In Review).

A new class of instruments, referred to here as lidar altimeters, developed at NASA's Goddard Flight Space Center (Bufton, 1989; Bufton et al., 1991; Blair et al., 1994; 1999; Garvin et al., 1998) have demonstrated a potential to greatly improve remotely sensed estimates of important aspects of canopy structure. These devices measure the vertical distribution of canopy structure using the principles of laser altimetry. The capability of traditional laser altimeters, which measure a single or several discrete ranges to a target, is expanded by recording the laser backscatter amplitude with very high temporal resolution. The approach yields a measure of the height distribution of illuminated surfaces within the laser footprint. Recent work has demonstrated that this measure can be used to accurately predict the total biomass of specific stands (Lefsky, 1997; Lefsky et al., 1999; Means et al., 1999) and the variability of forest structure (Lefsky et al., In Press) over a large range of biomass. In this paper, the measurement principles of lidar altimeters as applied to canopies and a validation of their ability to measure the height distribution of closed-canopy, broadleaf forests are presented.

Our interest in measuring canopy structure is motivated by the close relationship of many critical aspects of forest ecosystem function and structure to elements of canopy structure, defined as "the organization in space and time, including the position, extent, quantity, type and connectivity, of the aboveground components of vegetation" (Parker, 1995). Examples of important connections between function and structure are the dependence of: 1) the quality of biotic habitat on the volume of living space and stand heterogeneity, 2) stand microclimate on stand closure and gap sizes and frequency, and 3) the balance of energy and material fluxes with the lower atmosphere on the topography of the outer layer and total canopy surface area. The structure of the outer canopy has important functional implications, but the organization of the internal layers below the outer surface is likely even more important because it defines the distribution of a large surface area that exchanges gases (e.g., CO_2 and water vapor), absorbs and transmits radiation, and drags and diverts wind. Information on canopy structure has proved important for understanding the physiological activity of the entire canopy (Hollinger, 1989; Ellsworth and Reich, 1993), interception and retention of precipitation (Gash, 1979), radiation (Monsi and Saeki, 1953; Monsi et al., 1973; Brown and Parker, 1994), and atmospheric pollutants (Hicks et al., 1991), and the competitive interactions between forest trees (Horn, 1971). Brünig (1970; 1983) argued that the efficiency of ventilation and radiation absorption are strongly influenced by canopy structure. Surface irregularities may affect air exchange between canopy and overlying atmosphere (Meneti and Ritchie, 1994), and induce local wind patterns (Lowman and Wittman, 1996).

Canopy structure can also be a powerful predictor of conventional measurements of stand structure. At the most basic level, differences in stand development are reflected in the mean and maximum height of the canopy (Lefsky, 1997; Lefsky et al., 1999; Means et al., 1999). However, even for stands of similar height, the physical structure of canopies can vary considerably as a result of differences in the local importance of various mechanisms

of forest succession, disturbance, and environmental factors (Spies and Franklin, 1991). The effects of these processes may be discernible from subtler features of canopy structure, such as the height variability of the upper canopy surface and the volume of empty space within the canopy. These features of canopy structure have recently been used to predict aspects of stand structure such as the mean and standard deviation of stem diameter at breast height (DBH), the density of high DBH stems, and separate estimates of the basal area of shade-tolerant and shade-intolerant species (Lefsky et al., In Press).

Applications using canopy structure to assess forest ecosystem function or predict stand attributes are rare because existing ground-based approaches for measuring relevant aspects of canopy structure tend to be inexact, slow or highly averaged spatially. For example, the foliage height profile (MacArthur and Horn, 1969) provides information about the spatially averaged vertical distribution of leaf area, usually summarizing this characteristic over a large area of vegetation. This approach requires a large effort and is therefore usually only justifiable for whole-stand characterization. Though this approach provides valuable information on canopy structure (e.g., Aber, 1979; Aber et al., 1982; Hedman and Binkley, 1988; Parker et al., 1989; Brown and Parker, 1994) its typical use characterizing stand averages yields little information about the spatial variation of canopy structure.

The limitations of laborious ground methods and indirect, non-unique remote sensing techniques have restricted the use of structure observations in the study of canopies. Analysis of the backscatter signal recorded by lidar altimeters provides a compelling alternative for characterizing canopy structure. Because the technique rapidly and accurately measures the actual quantity of interest (i.e., height) in a direct and simple way it is better suited to measuring canopy structure than traditional ground-based or image-based approaches.

3.0 OBJECTIVES

The objectives of this work are to describe the general principles of the lidar altimeter method and to document the characteristics, validate the performance, and demonstrate the capability of an airborne lidar altimeter referred to as SLICER (Scanning Lidar Imager of Canopies by Echo Recovery). SLICER, developed at NASA's Goddard Space Flight Center (GSFC), is a scanning version of a profiling system that was explicitly designed to measure the vertical structure of forest canopies and the topography of the underlying ground surface (Blair et al., 1994). The specific objectives of this work are to: 1) describe the character of the raw SLICER backscatter signal, 2) present a method for transforming the raw signal into a canopy height profile (CHP) that quantitatively represents the vertical distribution of canopy components, 3) assess whether the measurements reveal, reproducibly, ecologically interesting variation in vegetation structure, and 4) test the similarity of the derived canopy height data to analogous measurements made from the ground in closed-canopy, broadleaf forest stands.

The description and validation of the SLICER canopy measurements given here provides the framework for the use of SLICER data in studies of forest canopy structure, including the work of Harding et al. (1994; 1995), Lefsky (1997), Lefsky et al. (1998; 1999; In Press), Harding (1998), Drake and Weishampel (1998), Means et al. (1999), and Rodriguez et al. (In Review) and for future studies. The principles developed here also apply to canopy lidar data being acquired by the airborne Laser Vegetation Imaging Sensor (LVIS) and to be acquired by the spaceborne Vegetation Canopy Lidar (VCL). LVIS is a wide-swath, mapping system developed at GSFC that has superceded SLICER (Blair et al., 1999). VCL, scheduled for launch in 2000, will sample canopy height and structure over approximately 5% of the Earth's land surface between ±67° during its 18 month mission (Dubayah et al., 1997).

4.0 BACKGROUND

The instrument and method we describe evolved from traditional laser altimeters. Systems employing a simple ranging approach have been used since the early 1980's to define canopy heights by measuring the elevation of the outermost canopy surface and, in some cases, the elevation of the underlying ground. This is accomplished by determining the round-trip travel time for the first and/or last detected return of a short-duration laser pulse. These ranging altimeter systems define the envelope of space bounded by the canopy top and the underlying ground. They employ small laser footprints with a diameter typically in the range 0.1 to 1 m, initially in a profile but more recently using scanning systems that image narrow swaths on the order of 100's of meters in width. Such altimetric canopy heights have been correlated, with varying accuracies, to a variety of vegetation attributes including tree and stand height (Schreier et al, 1984; Nelson et al., 1984; Ritchie et al., 1995; Naesset, 1997a; Magnussen and Boudewyn, 1998; Magnussen and Eggermont, In Review), timber volume and forest biomass (Maclean and Krabill, 1986; Nelson et al., 1988a; 1988b; 1997; Nelson, 1994; Naesset, 1997b), species composition (Schreier et al., 1985; Jensen et al., 1987), and canopy cover (Nelson et al., 1984; Ritchie et al., 1992; 1995; 1996; Weltz et al., 1994). These data have also been used to determine properties of vegetation not easily measured otherwise, including aerodynamic roughness length (Meneti and Ritchie, 1994), fractal scaling (Pachepsky et al., 1997; Pachepsky and Ritchie, 1998), and canopy complexity (Parker and Russ, In Review).

The first application in a study of forest canopies of an airborne lidar altimeter, recording the time-resolved amplitude of the backscattered laser pulse, was described by Aldred and Bonnor (1985). They evaluated the performance of a lidar system developed for bathymetric water depth sounding in order to assess its ability to measure forest canopy characteristics. They established the system's ability to determine stand height, closure, and type (hardwood, softwood, or mixed) for temperate forest stands in eastern Canada.

They found that the system measured stand height to an accuracy of ± 4.1 m with a 95 per cent confidence and that crown cover density was correctly classified in 20 per cent classes 62 per cent of the time. They concluded the measurements did not provide significant information on forest cover type. Nilsson (1996) evaluated a similar system, concluding that the lidar measurement underestimated mean height for pine stands in Sweden by 2.1 to 3.7 m. They also showed that a lidar prediction based on backscatter duration and amplitude was linearly correlated with stand volume up to the maximum volume observed (260 m^3/hectare). Spaceborne lidar altimeter techniques have been successfully demonstrated by the Shuttle Laser Altimeter (SLA, Garvin et al., 1998), an experiment intended to test hardware and algorithm approaches from orbit. SLA yields a measure of the total vertical roughness within 100 m diameter footprints which has been interpreted as canopy height in areas of low topographic relief (Garvin et al., 1998).

5.0 LIDAR ALTIMETER WAVEFORM CONCEPT

The lidar waveform is a record of the amplitude of backscattered laser energy received as a function of time (Figure 1). Unlike traditional lidar where returns from the entire atmospheric column are recorded at low vertical resolution, lidar altimeter systems record reflections only from the Earth's surface (in the absence of clouds). The return signal is recorded at very high vertical resolution, thus providing a finely resolved measure of the vertical distribution of illuminated surface area within the footprint, including plant area throughout the vegetation canopy. Where laser energy penetrates to the canopy floor and is reflected back to the receiver a measure of canopy height is obtained for that laser pulse from the travel-time between canopy top and ground reflections. Note that the laser energy decreases with depth through the canopy due to occlusion (reflection and absorption); less transmitted laser energy per unit area penetrates into the canopy with increasing depth. The amount of occlusion at a specific depth into the canopy is dependant on the amount of canopy area encountered higher in the canopy.

The intensity of the received backscatter return at a given depth in the canopy depends on the amount of laser illumination penetrating to that depth and on the reflectivity of the intercepted surfaces at the wavelength of the laser. Also, because the spatial distribution of laser energy is not constant across a laser footprint, the horizontal organization of reflecting surfaces with respect to the laser energy spatial distribution affects the intensity of the return (Blair and Hofton, 1999). In summary, the time history of backscatter energy is a measure of the vertical distribution of illuminated surface area, projected in the direction of the laser vector, weighted by the reflectance of the surfaces at the monochromatic laser wavelength and the spatial distribution of laser energy across the footprint.

It is important to note that the received laser energy reflected from the surface consists of returns due to single and multiple scattering events. Single scattering events consist of photons which encounter only one surface and which are reflected directly back to the receiver at 0° phase angle (parallel illumination and view angles; i.e., hot spot orientation). Multiple scattering events are comprised of photons that encounter more than one surface before being reflected back to the receiver, as can be the case for laser energy that is transmitted through foliage and subsequently is reflected from another surface. Laser energy reflected from the ground consists of singly-scattered photons, where a gap extends through the entire canopy to the ground in the direction of the transmit pulse, as well as some fraction of multiply-scattered photons. The path for multiply-scattered photons is longer than the straight-line path between instrument and target (the single scattering path) and thus those photons appear delayed in the waveform compared to singly-scattered photons. The amount of delay depends on the distance between scattering events and is thus a function of clumping of the canopy elements. The magnitude of the signal due to multiple scattering depends on the number of photons scattered back out of the canopy at 0° phase angle. A recent sturdy by Blair and Hofton (1999) comparing high-resolution,

small-footprint laser returns to return waveforms from a large-footprint lidar altimeter reveals no discernable multiple scattering contribution to the backscatter signal from dense, multi-layered, wet rainforest canopies in Costa Rica.

The relative strength of the canopy and ground returns provides information on canopy closure. We use the term canopy closure to mean the fraction of plant area per unit area, projected along the direction of the transmitted laser pulse. It is equal to one minus the gap fraction. The cumulative height distribution of canopy energy, normalized by the total return energy, is a relative measure of canopy closure as a function of height (Figure 1). The measure is relative because the reflectance of the surfaces encountered at 0° phase angle, at the wavelength of the transmitted laser pulse, determines the return signal strength from each surface, along with the range to the target and atmospheric transmission. Independent knowledge of the average reflectance of the canopy and ground surfaces within the laser footprint is necessary to convert the cumulative distribution to an absolute measure of canopy closure. The cumulative distribution also makes the simplifying assumption that only single scattering events contribute to the return signal.

6.0 SLICER CHARACTERISTICS

The SLICER airborne lidar altimeter system consists of a ranging component and ancillary instrumentation for geolocation. The ranging component consists of a laser transmitter, scan mechanism, receiver telescope, detector, timing electronics, waveform digitizer, and an instrument control and data collection system. The ranging instrumentation is augmented by an inertial navigation system for precise determination of laser beam pointing, GPS receivers for differential, kinematic determination of aircraft position, and video equipment for image documentation of the ground track. Integration of the ranging data with laser beam pointing and aircraft position yields a position and elevation for each laser pulse return with respect to a geodetic reference frame. Details of the instrument and

its operating characteristics pertinent to this work are described in Harding et al. (In Review).

Several aspects of the SLICER design make it a powerful tool for characterizing canopy vertical structure. The combination of a very narrow transmit pulse and a high-speed detector results in exceptional vertical resolution of approximately two-thirds of a meter, allowing closely spaced canopy layers and the underlying ground within each footprint to be distinguished in the backscatter return. Use of a very high-speed digitizer to sample the detector output results in a non-aliased waveform record of backscatter energy that has extremely good vertical sampling (11 cm), necessary for full analysis of waveform structure. SLICER evolved from a profiling lidar altimeter, originally described by Bufton et al. (1991) and subsequently enhanced by Blair et al. (1994), by the addition of a scanning mechanism. By scanning the laser footprints across the flight path a narrow swath results which provides cross- and along-track data from which information on canopy heterogeneity and ground slope beneath the canopy can be inferred. SLICER employs a higher power laser than is typical used by airborne laser altimeters that enables a significantly higher flight altitude (up to 8 km), yielding larger footprints (nominally 10 m but as large as 70 m) that are contiguous or even overlapped. The larger footprints fully illuminate the canopy, providing a measure of average canopy structure that avoids the sampling bias inherent to the spaced data points of small footprint altimeters. The canopy in these large footprints typically contains some openings at nadir to the ground thus consistently yielding a ground return and enabling a measure of vegetation height for each laser pulse. In addition, the high flight altitude minimizes the variation in footprint size and received backscatter energy caused by changes in ranging distance due to topographic relief, thus simplifying data interpretation. Accurate pointing and position knowledge and associated geolocation software (Vaughn et al., 1996; Hofton et al., In Press), enable accurate determination of the location of each footprint so that the lidar data can be directly

correlated with ground observations and georeferenced remote sensing images. SLICER's control systems and operational modes were designed to be flexible so that the effect of variations in footprint size, spacing and vertical sampling on characterization of canopy structure could be evaluated. Specific acquisition parameters used for this study are listed in Table 1.

Several implications of the instrument characteristics, described in detail in Harding et al. (In Review), are significant for proper use of the SLICER data. First, the laser illumination across the swath is not uniform and thus canopy structure across the swath is sampled unequally. The pattern of circular, approximately contiguous footprints that each have a radial, Gaussian distribution of laser energy yields a swath illumination that is analogous to an egg carton (Figure 2). Second, the backscatter amplitude recorded in the waveform is not an absolute measure of reflected laser energy due to varying atmospheric transmission and an uncalibrated transfer function between optical energy received by the instrument (i.e. backscattered photons) and the resulting digital count amplitude in the waveform. The transfer function varies spatially across the swath and temporally, on multiple time-scales, as operating conditions and instrument parameters vary (Harding et al, In Review). Thus, the amplitudes of waveforms can not be compared in an absolute sense. The waveform is most properly used as a relative measure of the height distribution of backscattered energy within an individual footprint.

Third, SLICER utilizes a threshold detection scheme to define the range to the first detected target within a footprint. Therefore, the detection of the canopy top requires that sufficient backscatter energy be received exceeding the detection threshold. The backscatter intensity depends on intercepted area and the near infrared (NIR) reflectance of the intercepted surfaces at 0° phase angle. Thus SLICER's ability to detect the canopy top, and the resulting derivation of canopy height, depends on the geometry of the outer canopy surface

and the reflectivity of the components making up the outer surface. For example, narrow, erect conifer tips with relatively dark needles at NIR wavelengths are less easily detected than a concentration of NIR-bright deciduous leaves forming a well defined, umbrella-like crown top. Depending on these canopy characteristics, the SLICER measurement of canopy height can be biased low by varying amounts compared to the outer-most canopy surface and, thus, stand-specific calibrations of canopy height measurements are necessary.

7.0 EXPERIMENT DESCRIPTION

The validation of the SLICER measurements of canopy structure is based on the transformation of the raw waveform record into a canopy height profile (CHP) using a method that accounts for the occlusion effect inherent to the lidar technique. The SLICER derived CHPs are then compared with ground-based, manually-observed height profiles for four forest stands of diverse structure. The ground-based approach is only appropriate for measurement of spatially-averaged characterizations of whole-stand vertical structure. Therefore, the validation is based on comparison of whole-stand structure using coincident ground and lidar data averaged over the same spatial scale. This validation is straightforward in that it compares the same type of observations (i.e., distributions of intercept distance). Furthermore, the observations from both SLICER and the ground are transformed to the canopy characteristic of interest (i.e., height profiles of vertical structure) using the same, simple methodology to account for the occlusion effect common to both sets of observations.

7.1 Study Sites

Work was carried out in four closed-canopy stands of very different vertical structure that represent stages in a successional sequence. They are separate stages of the "tulip poplar" association (Brush et al., 1980; Eyre, 1980), a mixed deciduous forest with overstory dominated by *Liriodendron tulipifera*. Specific stands were selected that have been the subject of previous studies of forest development and structure (e.g., Parker et al., 1989;

Brown and Parker, 1994). Three stands are within 5 km of each other, at the Smithsonian Environmental Research Center (SERC, 38°53'N, 76°33'W), about 10 km SSE of Annapolis, MD on the western shore of Chesapeake Bay (Figure 3). They include: a young stand with a narrow unimodal canopy, an intermediate-aged stand with a broad unimodal canopy, and a mature stand with a bimodal vertical leaf area structure. The fourth site is old-growth forest 20 km to the west (76°46'W, 38°54'N), known locally as the Belt Woods, that has a tall bimodal structure.

The young, intermediate-age, and mature stands were previously described by Brown and Parker (1994) where in the appendix they are referred to as 'crnb', 'kph4', and 'twrc', respectively. The young and intermediate-age stands developed after abandonment of a corn field and a pasture 13 years and approximately 40 years, respectively, prior to the collection of the data used in this study. The intermediate-age and mature stands are located within a forest at SERC for which a comprehensive stem map has been produced. The roughly square stem map area is approximately 600 m x 600 m in size. A grid system, referenced to the Maryland State Plane coordinate system, has been established with markers every 100 m. A meteorological flux tower is also located within the stem map area.

In each of the four selected sites stems greater than 2.0 cm DBH (vines, shrubs and trees) were measured, identified and classified for health in rectangular plots in 1995. The total area sampled ranged from 0.06, 0.1, 0.503, to 0.3 ha in the young, intermediate-aged, mature, and old-growth sites, respectively. The largest trees in each plot were cored with an increment corer and stand age was estimated as the number of rings in the oldest individual. The leaf area within each stand was measured by converting autumnal litterfall mass to leaf area. Leaves were retrieved from litter collectors from summer's end through the fall abscission period of 1995 at least once every other week to minimize decomposition

in the collectors. Leaves were sorted by species, dried to 60°C, and weighed. Species leaf areas were obtained from leaf masses using species-specific equations (e.g., Parker et al., 1989). One-sided leaf areas were summed by species to yield total collector leaf areas. Leaf area index was obtained as the leaf area collected divided by the total collector aperture. All the stands are completely deciduous. Details about the stand structure are given in Table 2. Stem information for the mature site comes from Parker et al. (1989) and LAI for the young and intermediate-aged sites from Brown and Parker (1994).

7.2 SLICER Data Acquisition

SLICER data was acquired for the four study sites on September 7, 1995 utilizing a T-39 Sabreliner jet based at NASA's Wallops Flight Facility, located near Chincoteague, VA. The canopies were fully leaved at this time, with no senescence having yet occurred (Parker and Tibbs, In Review). Latitude and longitude positions for the sites were preprogrammed in a real-time GPS flight navigator, enabling the aircraft pilots to fly transects that crossed the sites. A rosette pattern composed of six lines was flown across the large SERC stem map centered on the meteorological flux tower (Figure 3). The headings of the six flight lines were separated by 60°, yielding 12 radii extending outward from the flux tower. Aircraft roll caused local perturbations of the data ground tracks, up to several hundred meters off the flight track. One line each was flown across the young and old growth stands.

Each laser footprint was separately geolocated following the methods first described in Vaughn et al. (1996) and subsequently mondified by Hofton et al. (In Press). The accuracy of the SLICER geolocation at the footprint-scale was confirmed by a laser footprint located at the known position of the flux tower within the SERC stem map. The waveform for that footprint was inferred to include a return from the tower by the presence of a unique, distinctive, and anomalously high structure extending above the canopy top

equal to the known height of the tower (Figure 3). The position of the SLICER swaths was also confirmed by comparing time-stamped video frames of the ground track, acquired in-flight and co-aligned with the laser transmit beam, to canopy features in the field (e.g., dominant crowns and gaps). The horizontal offset between the SLICER ground tracks and the SERC stem map reported, and corrected, in Lefsky et al. (1999) is thought to be due to a reference frame discrepancy introduced during separate transformations of the two data sets to the UTM projection. Those transformations were not used here as they were not necessary for this study.

Transects of raw waveform return amplitudes, like that shown in Weishampel et al. (1996), were examined to identify segments of uniform backscatter character within each of the four study sites. For the intermediate-aged and mature sites within the SERC stem map grid, the field location of the uniform segments was established by converting footprint latitude and longitude to grid coordinates (WGS-84 to MD State Plane). Lacking field grids for the young and old-growth stands, the ground location of the uniform SLICER segments for these sites was established using the video records. Distinctive variations in canopy structure at these sites enabled accurate identification of the SLICER ground track in the field from the altimeter profiles and video records.

7.3 Ground Data Acquisition

The relative vertical distribution of leaf area was measured within two weeks after the SLICER flight in each stand along the selected lidar ground track segments using the method of MacArthur and Horn (1969), as modified by Aber (1978) and Parker et al. (1989). A 200 mm telephoto lens calibrated to measure distances was used to generate a distribution of the heights of the nearest surface above the observer to within 1 m resolution (in the old-growth stand, a 400 mm lens was also used for the occasionally very high leaves). Tree species identity and the type of tissue (leaf, bark, bud, flower, and seed) were recorded as well as the vertical height of interception. At each observation location

15 interceptions, arrayed in a 3 x 5 grid inscribed on the telephoto lens, were recorded. A grid of observation locations was established to systematically sample across the width of the SLICER data swath (e.g., Figure 4). The total number of interception observations was 615, 1020, 1260, and 1575 in the young, intermediate, mature, and old-growth sites, respectively, increasing as a function of stand height in order to provide an approximately equal number of observations per meter of height.

For this study, the interception observations for all surfaces (foliage and woody surfaces) were combined and transformed to yield a relative distribution of total plant area as a function of height (i.e., CHP). It is important to note that this method provides a relative plant area height distribution; it does not yield an absolute measure of total plant area (Brown and Parker, 1994). The transformation converts the distribution of intercept distances to the relative distribution of plant area by weighting the intercept observations in order to account for the effect of increasing occlusion with distance, following the Aber (1978) modification of the MacArthur and Horn (1969) method. The magnitude of the weighting increases with distances in a manner that depends on total gap fraction observed at nadir, defined by the proportion of clear-sky to interception sightings. The weighting at a given distance is larger for canopies with smaller gap fraction, accounting for the greater degree of occlusion in dense canopies. The gap fractions for these closed canopies were all small: young, intermediate, mature, and old-growth stands were 0.06, 0.05, 0.02, and 0.06, respectively.

8.0 DERIVATION OF SLICER CANOPY HEIGHT PROFILES

In order to derive canopy height profiles from the raw SLICER waveform distributions we adapted the transformation method applied to the ground-based sightings. Assumptions regarding canopy uniformity inherent to the transformation of the ground data (Aber, 1978) also apply to the transformation of SLICER waveforms. The horizontal distribution of canopy components within a layer is assumed to be random with respect to layers above

and below. In other words a Poisson distribution is assumed with no horizontal clumping of canopy components. Also, the leaf inclination distribution is assumed to be constant as a function of height so that the projected leaf area in the direction of observation (up-looking from the ground or down-looking for SLICER) is related in a constant way to total leaf area.

Several additional assumptions specific to the SLICER waveforms must also be made. To obtain an equivalent parameter to clear-sky sightings, that define gap fraction viewed upward from the ground, the proportion of ground return to canopy return signal strength is used. However, in order for this proportion to represent downward-viewed gap fraction, the ground return signal strength is modified in order to account for any difference in the average reflectance at 0° phase angle of the ground and canopy at the laser wavelength. In most circumstances this ratio between ground and canopy reflectance is not known at the scale of the laser footprints and a value must be estimated. Application of the method to SLICER waveforms also assumes that the reflectance of the canopy components is constant as a function of height. Whereas for the ground sightings each canopy intercept counts equally in the resulting distribution, for SLICER an equivalent surface area contributes greater return signal as reflectance increases. This assumption inherently implies that the ratio of woody to leafy surface area and the woody and leafy reflectance are constant as a function of height. Finally, it is assumed that multiple scattering, causing lengthened photon travel paths, does not contribute significantly to delayed signal in the waveform, because either the amount of multiply-scattered photons received in the backscatter direction is small compared to singly-scattered photons or the magnitude of any resulting delay is small. Implications for each of these assumptions are considered in the discussion section.

Applying the above assumptions, a sequence of processing steps transforms the raw waveform into a CHP (Figure 5), extending the methods reported in Lefsky (1997). First,

to improve the signal-to-noise ratio of the distribution the raw digitizer count amplitudes (Figure 5a) are summed by accumulating the signal in adjacent waveform bins. Here, 6 adjacent bins are summed, yielding a 66 cm vertical sampling which is approximately equal to the vertical resolution defined by the laser pulse width and detector response. Next, the mean and variance of the background noise are established using the final portion of the waveform, beyond any potential last ground return. The mean background noise is subtracted from the summed distribution yielding signal above the noise level (Figure 5b). Negative results, where the variance in the noise causes the waveform signal to be less than the mean noise, are set to zero.

We then distinguish the ground reflection in the signal by assuming that it is the last return above noise. The end of the last return is defined as the latest signal above a threshold that is a multiple of the background noise variance (Figure 5b). The peak of the last return is defined to be the first inflection in signal strength prior to the end of the last return, identified using its first derivative. The start of the last return can not be uniquely identified from the raw distribution because backscatter return from low vegetation could be convolved in time with the ground return. Therefore, the start of the last return is identified based on the width characteristics of the system impulse response. The impulse response is the theoretical signal recorded from a smooth and flat surface and depends on the convolved effects of pulse width and detector response. The SLICER impulse response is established from minimum-width returns from water surfaces. A ratio is determined for the impulse response between the width from the signal end to peak compared to the width from peak to start. The observed end-to-peak width of the last return is scaled by this ratio in order to define the start position of the last return. This method accounts for any pulse broadening of the last return due to slope or roughness of the ground within the footprint. After automated identification of the last returns, the results are interactively evaluated, and modified where necessary, by examining the raw waveform, with the last return identified,

along with profile plots of last return start, peak, and end elevations. Anomalous variations in elevation or last return width, either along or across the SLICER swath, reveal improperly identified ground returns that are then manually corrected on the raw waveform.

The amplitude of the identified ground reflection (area under the curve above mean noise) is scaled to account for the difference between average canopy and ground NIR reflectance at 0° phase angle. For this work the ground return amplitude was increased by a factor of two based on the assumption that the reflectance of the ground, dominantly comprised of leaf-litter with some bare soil and rare live foliage, was half that of the canopy. A factor of two was chosen based on typical NIR reflectance spectra of leaf-litter and soil versus deciduous foliage. However, reflectance data for these specific sites were not available. Furthermore, measurements of average background and canopy reflectance specific to the lidar altimeter technique, at 1064 nm and 0° phase angle, for closed-canopy, deciduous forests are not available in published literature. However, the results of this work are relatively insensitive to potential errors in this reflectance scaling factor, as described in the discussion.

A cumulative height distribution for the canopy return is then calculated, normalized by the adjusted total return (canopy + scaled ground), yielding a height distribution of canopy closure (Figure 5c). The effect of occlusion is corrected by weighting this distribution by [-ln(1-closure)] (MacArthur and Horn, 1969; Aber, 1978), transforming the result to a cumulative distribution of plant area projected in the direction of the laser beam (Figure 5c). The cumulative distribution is normalized and converted to an incremental height distribution, yielding the CHP which depicts the fraction of total plant area per measurement interval (Figure 5d). The height of the CHP intervals are referenced to the start of the ground return. Comparing Figure 5a to 5d, one observes that signal at greater depths into the canopy is proportionally increased by the weighting that accounts for occlusion. The degree of weighting with depth increases as a function of closure. This

method of establishing the relative height distribution of plant area, depending only on the relative amplitude distribution within a single waveform, is consistent with the varying and uncalibrated relationship between waveform amplitude and received backscatter energy for SLICER. There is no dependence on absolute backscatter energy and no comparison of energy amplitude between laser shots is made.

9.0 REPRODUCIBILITY OF SLICER CANOPY HEIGHT PROFILES

As a test of the reproducibility of the SLICER-derived CHPs, the results at ground track intersections are compared for 6 locations within the SERC stem map (Figure 6). At four locations two ground tracks overlap and at two locations three ground tracks overlap. This reproducibility test is an end-to-end check of the SLICER system, evaluating the integrated system components (instrumentation, geolocation methodology, and CHP processing algorithms). Five of the intersection areas occur entirely within the mature stand with a bimodal vertical leaf area structure. One intersection is dominantly within the mature stand but partly includes the intermediate-age stand with a broad, unimodal vertical structure. Laser footprints within the areas of overlap were identified and CHPs were computed for each. The footprint CHPs within an overlap area for each flight line were averaged together, yielding an average CHP per line. The average CHPs for each flight line in an intersection area are compared in Figure 7.

The CHPs at each intersection show remarkable agreement, with specific features of the distributions consistently reproduced. Each intersection area yields a bimodal distribution. Furthermore, the height above the ground, the width, the 'peakedness', the amplitude of each mode, and the amplitude and height of the minimum between the modes are systematically reproduced, with only a few minor exceptions (height of the higher mode at the lines 2-4 intersection and amplitude of the lower mode at the lines 2-3-5 intersection). The maximum height of the CHPs also agree to within 1 meter or better, and the initial

slope of the distribution from the maximum height to the peak of the upper mode is very uniform, except for the lines 2-4 intersection. Some of the footprints in the area of overlap between lines 2 and 4 resulted in waveforms which lacked any recognizable ground return, probably due to nearly complete or complete canopy closure. These footprints were excluded from the derivation of the average CHPs, yielding CHPs representing slightly different areas that probably accounts for the discrepancies seen at this intersection.

Not only are the CHPs reproduced at each intersection, but variations between intersections are revealed. The maximum height, the initial slope, and the height, width, peakedness, and amplitude of the modes vary from location to location. The relative size of the lower modes compared to the upper modes markedly vary between locations, as does the amplitude of the minimum between the modes. The variations, though in some cases subtle, are greater than the differences between repeat CHPs at a single intersection location indicating that the variations are reproducibly detected. In some cases the variation between locations is occurring over a spatial scale that is only two or three times larger than the over lap areas from which the CHPs were derived. For example, the distance between intersections 1-3-4, 2-4, and 2-3-5 is at most 150 m (compared to overlap widths of 50 m), yet differences are observed between these locations, particularly in amplitude of the lower mode and the peakedness of the upper mode.

We interpret the SLICER-derived, average CHPs to be a measure of canopy vertical structure. The maximum height of each distribution is interpreted to be the height of the upper-most detected canopy component within the sampled area (i.e., maximum canopy height). The upper and lower CHP modes are interpreted to correspond to the canopy overstory and understory. The area of each mode is a measure of the relative plant area of the layers and the widths of the modes correspond to the layer depths. The decrease between the modes corresponds to a relative absence of plant area between the stories (i.e.,

a midcanopy gap), with the amplitude being a measure of the sparseness within the gap. The initial slope of the CHP is inferred to be a measure of the ruggedness of the outer canopy within the sampled area. Flatter slopes correspond to a more planar outer canopy.

The spatial variation observed in the average CHPs is interpreted to be a measure of the spatial variation of canopy structure. The scale of the spatial variation is revealed in transects across the four study sites depicting CHP results for individual laser shots along a single, cross-track beam position within the SLICER swath (Figure 8). The young site, with a very uniform, unimodal CHP structure, is a narrow stand bounded on the southwest by a riparian forest and on the northeast by a corn field which had a mature, standing crop at the time of the SLICER flight (Figure 8a). The riparian forest, bordering a stream channel, was the site of nitrogen uptake studies conducted by Peterjohn and Correl (1984) and Jordan et al. (1993). The structure of the stand to the northeast of the corn field was described by Brown and Parker (1994, Carbon 1 stand) as unimodal and lacking an understory. The intermediate-age stand has a uniform maximum height and, in general, consists of a relatively broad overstory and a minor to absent understory (Figure 8b). However, a 30 m wide section within the middle of the stand consists of a uniformly distributed CHP throughout the height of the canopy. The ground sampling plot (gsp) includes both this segment and the more typical, broad overstory structure. The mature stand is, on average, taller than the intermediate-age stand but has a more variable maximum height (Figure 8b). The mature CHPs show a bimodal structure with a narrow overstory, a midcanopy gap, and a pronounced understory. The magnitude and depth of the understory varies spatially, consistent with the variable understory in the average CHPs at the intersection areas (Figure 7). The old-growth stand is tall with a variable maximum height, a relatively narrow overstory, a broad midcanopy gap, and a pronounced but variable understory (Figure 8c). Significant understory development occurs where 20 to 30 m wide gaps are present in the overstory (at 280 m and 350 m in Figure 8c).

10.0 COMPARISON OF SLICER AND GROUND CANOPY HEIGHT PROFILES

The validity of the SLICER CHPs was assessed by comparing average SLICER and ground-based CHPs for the set of SLICER footprints that overlap with the ground sampling grids at the four study sites. Because the right-most footprints in the SLICER swath had significantly lower signal-to-noise than the other four cross-track footprint positions, these footprints were not included in the derivation of the average SLICER CHPs. The low signal-to-noise for the right-most footprints was probably due to misalignment between the footprint scan pattern and the receiver field-of-view, described in Harding et al. (In review). In addition, the central part of the mature site ground sampling plot, which was crossed by flight lines 2 and 4 (Figure 6), contained some of the footprints in both flight lines which lacked any recognizable ground return. A composite of non-overlapping footprints with valid ground returns was created from the two flight lines in order to derive a CHP that maximized the SLICER coverage across the ground sampling plot. Ground grid points for the mature site lacking coverage by valid SLICER footprints were excluded from the ground CHP. A total of 16, 24, 12, and 79 footprints were used in the derivation of the average SLICER CHPs for the young, intermediate-age, mature, and old-growth stands, respectively. For each site, the ground and canopy returns were first summed for all the footprints, referenced in height to the start of the ground return, prior to computation of the average SLICER CHPs using the methodology described above for a single footprint. SLICER CHPs were computed with a 1 m vertical binning to be comparable to the binning of the ground-based CHPs.

Comparisons of the SLICER and ground CHPs are shown in Figure 9. Un-transformed distributions of vertical interceptions made using the ground observations and of the vertical distribution of canopy return energy from SLICER (left panels, Figures 9) shows each datasets' bias towards shorter distances, due to the occlusion effect. Occlusion results

in a bias towards lower observations in the upward looking ground observations, and a bias towards higher observations in the downward looking SLICER observations. In contrast, transformation of the raw data, via the MacArthur-Horn algorithm (center panels, Figure 9), results in ground and SLICER CHPs whose general features are in agreement. The stand heights for both the ground and SLICER results increase in successional sequence from young to old-growth. For the shorter, unimodal young and intermediate-age stands, both the vertical position and maximum relative plant area in the single overstory peak is qualitatively in agreement. In addition, the decrease in relative plant area observed at heights both above and below the peak define slopes in the SLICER CHPs that are comparable to the ground CHPs. For the taller, bimodal mature and old-growth stands, the location and width of the understory peaks, a midstory decrease in the relative density of plant area, and the presence of a broad overstory are all similarly identified in the SLICER and ground CHPs.

Differences between the SLICER and ground measured CHPs do exist (Table 3). All of the SLICER CHPs are taller than the corresponding ground CHPs, by between 7 and 12% (between 2 and 4 m). With one exception, the mean height of the SLICER CHPs was also higher, by between 5 and 11% (0.9 and 2.2 m). The mean height of the SLICER CHP for the young plot was 9% (1.0 m) lower than the corresponding ground CHP. For the stands with a single clearly defined mode (young, intermediate-age) the height of the peaks (defined as the height at which the fraction of plant area in a height interval is at a maximum) in the ground and SLICER CHPs are within 3 m of each other. The SLICER CHPs result in a lower relative plant area at the peak height, underestimating this quantity by 33% in the young plot and 43% in the intermediate-age plot compared to the ground CHPs.

Assessing the SLICER to ground agreement of the two taller, bimodal stands (mature, old-growth) is more difficult. The overstory of the mature stand is very broad (25 m) and lacks a single well defined peak in both the ground and SLICER CHPs. Instead, the overstory in both CHPs is composed of several small sub-peaks. There is good qualitative agreement between the upper story depth and relative plant area amplitude in the ground and SLICER CHPs. The understory of the SLICER CHP has two sub-peaks that bracket a single peak in the ground CHP, and SLICER underestimates the maximum relative plant area of the understory by 33%. In the old-growth stand, the overstory in the ground CHP is significantly broader (25 m) and composed of multiple sub-peaks compared to a single-peaked, narrower (15 m) overstory in the SLICER CHP. The difference in height between the SLICER and ground overstory maxima is about 5 m. The height of the SLICER CHP understory peak is about 1 m above the corresponding peak in the ground CHP, and SLICER estimates the maximum relative plant area of the understory to be 14% less than in the ground estimate.

The quantitative goodness-of-fit of these two estimates of each stand's CHP has been evaluated in two ways. First, a root-mean-square difference has been calculated between the SLICER and ground CHPs for each stand. For comparison, a second RMS difference has been calculated between CHPs using two subsets of the ground data, made by separating evenly and oddly numbered ground collection points. For the young to old-growth succession, SLICER versus ground and ground versus ground RMS differences are 0.014, 0.012, 0.008, 0.009 and 0.028, 0.020, 0.014, 0.011, respectively. In every case, the RMS difference between the SLICER and ground data is less than the RMS difference between the two subsets of the ground data.

To test the statistical significance of these results, a Chi-square goodness-of-fit test was performed. In order to execute this test, which depends on the number of observations in

each distribution, the CHP vectors had to be transformed into vectors of count data, rather than the normalized CHP distribution data. For the ground CHPs, vectors of counts were generated by multiplying the relative CHPs by the total number of ground observations. For the SLICER CHPs, a number of considerations had to be addressed before a sample size could be determined. The motivation for this determination of sample size is the higher statistical power, in the Chi-square test, associated with larger number of observations. If the number of observations is inflated, a higher probability of rejection will be obtained than is justified. The individual observation recorded by the SLICER system is the digitizer count, which represents an unknown number of individual received backscatter photons. Given the large number of digitizer-count observations (>4000 above background noise level) which are made over a 10 m footprint, it is likely that each observation represents a smaller area than is observed by the human operator making ground measurements. As a result, it is probable that each ground and ground observation are not equivalent for statistical purposes. Previous work (Lefsky, 1997) has indicated that there was no statistically significant difference between CHPs made using a 10% subset of digitizer counts from a waveform and CHPs made from all the observations from the same waveform, indicating that, for the purposes of making CHPs, SLICER digitizer counts are an over-sample relative to the amount needed to describe the canopy.

We first tested whether CHPs could be made using a subset of the SLICER digitizer counts whose number was equal to the number of ground observations for a site, without the Chi-square test detecting a statistically significant difference between the sub-sampled SLICER CHPs and those created using the full waveforms. To create CHPs using the full waveforms, all SLICER waveforms for each study site plot were first transformed into CHPs and the CHPs were then averaged. Then for each waveform in each stand, the ground return was removed, using the methods detailed above, and the resulting vectors were sub-sampled and all sub-samples were then pooled and then transformed using the

MacArthur-Horn method. The number of subsamples for each waveform was set so that, when the subsamples for all waveforms in each stand were accumulated, they summed to the number of ground observations for the same stand. A Chi-square uneven-sample-size goodness-of-fit test was performed to determine whether significant differences existed between the CHPs made with the sub-sampled and full waveforms (Table 4). No statistically significant differences between the two SLICER CHPs were found.

Because differences between CHPs created with the full and subsampled SLICER waveforms were not significantly different, subsampled waveforms were used for subsequent analysis so as to not bias the Chi-square results with an inflated sample size. An even-sample Chi-square goodness-of-fit test was performed to test whether the ground and SLICER estimate of the CHP were significantly different (Table 5). For each stand, there were statistically significant differences between the two estimates. RMS differences between ground and SLICER CHP were recalculated, using the sub-sampled estimates of the SLICER CHP. The RMS values were similar, but lower, than those obtained with the full set of SLICER data; the RMS differences for the SLICER-ground comparison were less than or equal to those for the ground-to-ground comparison.

11.0 DISCUSSION

The major characteristics of the SLICER and ground CHPs show good agreement for each stand and both document the same changes in structure in the successional sequence from young to old-growth, closed-canopy, broadleaf forests. These general similarities between complimentary, but differently implemented, measurements of canopy intercept distances suggest that both the SLICER and ground CHPs accurately depict the basic vertical structure of these stands. Furthermore, the comparison of average SLICER CHPs at flight line intersections demonstrates that SLICER depicts the canopy structure in a highly reproducible way. Despite the good general agreement between SLICER and ground CHPs, specific aspects of the CHPs exhibit statistically significant differences, as indicated

by the Chi-square tests. These differences are likely due to characteristics of the SLICER instrument and ground sampling strategy, and due to differences in how the methods interact with the canopy structure. These differences point to potential inaccuracies in the methods and to limitations in the generality of these results for other forest types. In the following sections we examine these differences and evaluate how they might affect the comparison and the utility of the methods.

11.1 Measurement Effects

Several factors cause the ground CHPs to be noisier and discontinuous compared to the SLICER CHPs (Table 6a). First, the grid of ground measurement locations samples a small fraction of the canopy within the field plot area (Figure 4) whereas the SLICER 'egg carton' illumination pattern fully samples the plot, although unevenly (Figures 2 and 4). Second, the accuracy of the camera method for determining distances to the first interception falls of rapidly with height (Lefsky, 1997), whereas the SLICER distances have constant accuracy (11 cm). Third, because of the significant effort required to make the manual observations, the ground approach has only a small fraction of the observations per CHP compared to SLICER, resulting in a relative undersampling by the ground method. Fourth, occlusion of farther targets by nearer ones, a feature of both methods, causes a reduction of intercept observations at greater distances (Figure 9), yielding SLICER CHPs that are noisier low in the canopy and ground CHPs that are noisier high in the canopy. However, because the ground method consists of far fewer observations than SLICER, this effect is significantly more pronounced for the ground CHPs. As each of the small number of overstory ground observations represents a great deal of leaf area following application of the MacArthur-Horn transformation, the result is a noisy measure of overstory structure. Fifth, differences between the methods in the discreteness and dependence of the raw observations are also reflected in smoothness of the transformed estimates of canopy structure. SLICER returns are continuous but dependent (correlated)

over a height resolution that is approximately two-thirds of a meter and the derived CHPs are thus also continuous and somewhat smoothed. The ground intercept sightings are discrete and independent, yielding CHPs that can be discontinuous and stepped.

The overall effect of these measurement properties, yielding ground CHPs that are noisier and discontinuous compared to the SLICER CHPs, accounts for part of the observed statistical differences. The ground CHPs exhibit large variations in relative plant area from bin to bin compared to the smoother SLICER CHPs, especially higher in the canopy (Figure 9). The few ground observations high in the canopy, and resulting empty CHP bins, accounts for the consistently lower maximum canopy height in the ground CHPs; the highest part of the canopy was not observed from the ground due to occlusion whereas SLICER is most sensitive to plant area at the top of the canopy. The noisier, undersampled character of the ground CHPs is indicated by the RMS comparisons in which the SLICER CHPs are more like the ground CHPs, in three of four cases, than are the ground subset CHPs to one another. Lefsky (1997) showed statistical similarity between the SLICER CHPs and smoothed versions of the ground CHPs based on Chi-square tests, further indicating that the statistical differences reported here are, in part, due to the comparatively noisy character of the unsmoothed ground CHPs.

11.2 Canopy Effects

Departures from the assumptions of canopy uniformity cause height biases in the ground and SLICER CHPs (Table 6b). Three canopy properties affect both the ground and SLICER CHPs. First, horizontally non-random distribution of canopy elements (i.e., clumping) will bias the two methods in opposite senses. Clumping of foliage implies greater foliage-free distances than for uniform situations; that is, laser energy will penetrate deeper into the canopy from the SLICER point of view, whereas for the ground method the upward distance to the first intercept will be longer. Thus, the assumption of horizontally

random canopy elements will cause the SLICER CHPs to be biased high and the ground CHPs to be biased low for canopies which in fact exhibit clumping. Second, leaf inclinations for these canopies are not uniform as a function of height but in fact change from nearly flat (planophile) in the lower canopy to more vertical (erectophile) in the upper canopy (Parker, unpublished data). This change in leaf inclination yields fewer ground-observed intercepts and less SLICER backscatter energy per unit of total leaf area with increasing height in the canopy. Both methods are consequently biased to lower canopy heights.

Third, where there is much spatial variation in maximum canopy height ("rugosity" in the sense of Parker and Russ, In Review), the intercept distances of tall canopy locations are mixed with those of adjacent shorter areas. For the upward looking ground observations, this results in a too small weighting of the distant foliage, and therefore a CHP that is biased downwards. For the downward looking SLICER observation, the majority of the energy returned to the sensor comes from the uppermost layer of canopy, whether the maximum canopy height is planar or variable. In the planar canopy, the high power return comes from a relatively uniform layer at the top of the canopy, and the reduction in return energy due to occlusion decreases in a horizontally uniform way. In the case of variable maximum canopy heights, the high energy return is distributed throughout the range of the upper canopy surface height. As a result the CHP is biased in the direction of the mean plant area height. In these closed canopy cases where the mean canopy height is below the average height of the outer-most canopy surface, the SLICER CHP is biased downwards.

Three canopy properties affect only the transformation of SLICER observations to CHPs (Table 6b). First, the application of the MacArthur-Horn transformation requires an estimate of the gap fraction to account for the occlusion of far surfaces by near ones. In the ground method the gap fraction is determined directly by the proportion of clear-sky

sightings, but for SLICER it depends on separation of the ground and canopy returns and scaling the ground return to account for NIR reflectance differences. Due to the lack of appropriate reflectance values for the sites in this study, a canopy to ground reflectance ratio of two was assumed for all four sites. Table 7 compares the ground-observed gap fraction with SLICER gap fractions using canopy to ground ratios of 1 and 2, and reports the ratio required to produce a SLICER gap fraction equal to that observed by the ground method. The large range in required ratios, from less than 1 to greater than 2, is not realistic for these similar canopies (closed, deciduous-only) with uniform ground cover indicating inaccuracies in the SLICER and/or ground determinations of gap fraction. However, for high-closure canopies the derivation of CHPs is relatively insensitive to errors in gap fraction, and thus to errors in the assumed canopy to ground reflectance ratio. Figure 10 shows average SLICER CHPs for the four sites computed using ratios of 1, 2, and 4, corresponding to ground reflectance equal to, one-half, and one-quarter that of the canopy. The effect on the distributions is minor, but assumption of a ratio of 2 causes a small upward bias when the ratio is in fact less and a small downward bias when the actual ratio is larger.

A second canopy property affecting the SLICER CHPs is the vertical distribution of canopy reflectance, which is assumed to be constant in the transformation method. Studies of broadleaf reflectance as a function of vertical position within canopies are rare, with the few results showing no significant within-species differences between upper and lower canopy leaves at NIR wavelengths (Middleton et al., 1998; Demarez et al., 1999). However, NIR leaf reflectance can change with height due to changes in species composition between stories; Middleton et al. (1998) document an upward increase in foliar NIR reflectance for three of four boreal forest stand types examined. A likely increase in the proportion of foliar versus woody surfaces upward through canopies is also likely to cause canopy NIR reflectance to increase upward (e.g., Huemmrich and Goward, 1997).

Plant area in SLICER CHPs will be biased high in cases where NIR reflectance increases upward.

Finally, while the meaning of distance is unambiguous in the ground method, some SLICER distances may reflect a lengthened photon travel path within the canopy due to multiple scattering. Any multiple scattering contribution to the waveform will cause the derived SLICER CHP to be biased low. The canopy undoubtedly causes significant scattering of the laser radiation, especially due to the high transmittance of deciduous leaves at NIR wavelengths. However, because the laser beam is highly collimated and the receiver has a very narrow field of view, we expect a relatively small fraction of the received backscatter returns to be multiply scattered. The path delay for those returns that are multiply scattered will depend on the spatial position (i.e., clumping) of the reflecting surfaces, and may be minor for closely packed foliage. Qualitative observation of individual, raw SLICER waveforms suggests that increased path length due to multiple scattering is minor, indicated by the presence of narrow vertical gaps within the canopy return where backscatter energy decreases to the background noise level and by the absence of a significant tail of multiply scattered return energy occurring later than the ground return.

In light of the many possible ways that instrumentation, sampling methods and interactions with canopy organization can influence the perception of structure through intercept distance measurements, it is remarkable that the ground and SLICER methods yield CHPs that are so similar. Either the effects we have listed are all relatively small or in some way are negatively correlated and cancel each other. It is difficult to ascribe relative importance to the effects in Table 6b causing potential bias in the CHPs. Because the offset of SLICER to ground CHP means increases upward as stand height increases (Table 3), it might be inferred that effects that bias the SLICER results upward and/or the ground

downward predominate. However, examination of the ground to SLICER CHP comparisons (Figure 9) shows that much, if not all, of the increasing offset in the means is due to the increasing under-representation of the upper canopy by the ground method as stand height increases. The under-representation of the upper canopy is likely caused by the difficulty in observing upper-canopy surfaces from the ground and the low total number of ground observations (Table 6a), rather than by errors introduced by the assumptions of canopy uniformity (Table 6b).

We suspect that of the canopy properties affecting the derived CHPs (Table 6b) non-random horizontal clumping is the largest source of error for closed-canopy, broadleaf forests. Canopies can depart significantly from the assumption of a horizontally random, Poisson distribution of surfaces. However, a coupled scattering and receiver model specific to the parameters of the lidar instrument (e.g., collimated, monochromatic, NIR illumination and very narrow receiver field-of-view) is required to quantitatively evaluate the effect of each of the canopy properties. An initial model incorporating artificial forest scenes, composed of individually generated trees, a Monte Carlo ray tracing radiative transfer model and a SLICER-like lidar receiver was used to evaluate the potential contribution of multiple scattering path delay to the waveform as a function of canopy closure (Govaerts, 1995). Results showed larger path delays than are empirically observed in the SLICER waveforms, possibly due to an underestimate of short-range scattering events caused by the elimination of closely clumped leaves, twigs, stems and branches from the target scenes to simplify computations. Refinement of radiative transfer models incorporating realistic scene and instrument properties is a necessary step to evaluate the relationship between canopy characteristics and lidar backscatter signals.

11.3 Application of the Results

There are some limitations in the domain over which these results can be applied and in the meaning that can be associated with the derived structure information. The current test has been restricted to broadleaf, deciduous forests with restricted variation in cover (> 90% closure) and overstory species composition. However, within these conditions we found correspondence of ground and lidar measurements for stands of varied biophysical characteristics (gap structure, stature, relative distribution of canopy surface) and we feel the lidar method will apply generally to closed-canopy, broadleaf forests. Direct application of the CHP methodology to other sorts of canopies may not be appropriate. Other canopies can depart more significantly from the assumptions of uniformity than the stands we tested. In particular, open woodlands and stands of cone-shaped crowns strongly depart from the assumptions of random horizontal organization (no clumping) and uniform height of the canopy outer surface within the laser footprint. In addition, the CHP bias due to error in the ground reflectance scaling factor increases with decreasing canopy closure because of greater error introduced in the [-ln(1-closure)] transformation weighting function. An error in scaling factor causes an error in closure which is larger, in an absolute sense, for open canopies compared to canopies with high closure.

The ecological meaning of the CHP method is closely linked to the scale of the footprint. In this present case, with a 10 m footprint, the CHP for a laser shot reflects a canopy scale, not the influence of individual crowns. We do believe the method does provide meaningful information at the 10 m scale. Although our test strictly compared averages of derived structures from spatially distributed laser footprints and ground based measurements, it is unlikely that the average distributions could be similar without a great deal of correspondence in the components of the average. Furthermore, Figure 8 shows consistent and understandable variation along CHP transects, which also suggests that the individual shots have physical reality and ecological meaning.

It also must be remembered that the SLICER CHPs provide not the absolute height distribution of canopy surfaces, but the relative one; that is, the fraction of the total plant area within height intervals. It is not possible to predict the total amount of plant area from either the ground-based sightings or SLICER measurements (Aber, 1978; Lefsky, 1997). The total absolute plant area of a stand, obtained by other means such as leaf litter collections, must be combined with the SLICER relative CHP to yield an absolute height distribution. Furthermore, the SLICER return gives no information on the character of the reflecting surfaces in terms of the type of tissue (foliage or bark), its state (alive, stressed or dead), or the species. The traditional foliage height profile (Aber, 1978) derived by the ground-based sighting observations, although manually intensive and thus spatially limited, can be used to provide important information on tissue type, state, and species (e.g., Brown and Parker, 1994) not achieved with the lidar method. The laborious nature of the ground observations does limit the number and spatial scale of stands that can be characterized, and thus only a few stands were compared in this work. Validation of airborne and spaceborne lidar observations would greatly benefit from a field-portable, up-looking laser ranging system than could rapidly and accurately characterize canopy vertical structure at multiple spatial scales along lidar ground tracks.

Unlike many more familiar products of remote sensing, SLICER yields neither a map nor an image - instead it provides detailed vertical information along a linear path. Along this transect it provides essentially volumetric information on the distribution of optical reflecting elements, a sort of information not available from traditional image-based products. Moreover, this linear sampling limitation can be overcome: the LVIS instrument (Blair et al., 1999), the airborne successor to SLICER, has a broadened swath width, as wide as 1 km, and significantly improved amplitude calibration of the backscatter return energy.

12.0 CONCLUSIONS

The lidar altimeter instrument and methodology we describe provides information about canopy vertical structure that is closely related to similar measurements taken from the ground for the same portion of canopy: it reproduces the overall stature and the height of the principal modes in the distribution of plant area. In the same forest type the method distinguishes different canopy structural types, found from a comparison among developmental stages. Structure is distinguished with a sensitivity on the spatial scale of the size of overstory trees, as revealed in transects through differing structural types. Moreover, the method is reproducible: repeat measurements of the same locations give essentially the same vertical distributions. Together these characteristics validate a system that obtains information of considerable ecological value about the organization of a major component of the biosphere.

Although the lidar and ground-based measures of canopy vertical structure similarly characterize the structural variations between the four stands studied, there are statistically significant differences between the CHPs for individual stands. These differences are in part a consequence of the atrributes of the data, with SLICER resulting in smooth, continous, very well sampled distributions and ground observations resulting in stepped, discrete, less well sampled distributions. This is especially the case high in the canopy where ground-based sightings are rare, typically resulting in an underestimate of canopy surface area and height as compared to the SLICER results. Departure from the assumptions regarding canopy properties used to transform raw observations to surface area height distributions may also lead to differences between the SLICER and ground results. In particular departures from the assumption of horizontal randomness caused by clumping bias the distributions toward the observer, upward for SLICER and downward for ground-based CHPs.

The sensitivity and spatial resolution of SLICER may aid in assessing important aspects of spatial variation in vegetation, including gap structure, stand complexity and structural diversity. The footprint size (nominally 10 m) was chosen to reflect the size of the characteristic canopy element: it is large enough to capture the local maximum height of an assemblage of tree crowns and yet small enough to reliably differentiate ground and canopy contributions to the waveform. This is an important scale in forest dynamics in mature stands because it is the typical size of the canopy hole produced when a tree falls. Studies of the structure of vegetation at spatial scales on the order of 10 m have not, to date, been possible with traditional remote sensing methods.

13.0 ACKNOWLEDGEMENTS

This work was supported by the Terrestrial Ecology Program of NASA's Earth Science Enterprise, the NASA Global Change Fellowship program, and the Smithsonian Environmental Sciences Program. The work was performed at NASA's Goddard Space Flight Center, the University of Virginia, the USDA Forest Service Pacific-Northwest Research Station, and the Smithsonian Environmental Research Center. Development of the SLICER instrument was supported by NASA's Solid Earth Science Program and the Goddard Director's Discretionary Fund. SLICER data sets available for public distribution are documented at http://denali.gsfc.nasa.gov/lapf. We thank David Rabine and Barry Coyle for operation of the SLICER instrument and Earl Frederick and Bill Krabill for assistance in GPS operations. The Aircraft Programs Branch at Goddard's Wallops Flight Facility conducted the aircraft flight operations for the SLICER data acquisition, and Wayne Wright provided the flight navigation software. Michelle Hofton made improvements to the geolocation software developed by one of us (Blair) and Melanie Taylor and Kathy Still applied the SLICER geolocation processing. George Rasberry and Donna Tibbs conducted the ground-based foliage profile measurements. Dr. Lefsky also thanks Drs. H.H. Shugart, B.P. Hayden, J.H. Porter and W.B. Cohen for their assistance. We thank Jon Ranson, Jim Smith and anonymous reviewers for constructive comments that improved the manuscript.

14.0 LITERATURE CITED

Aber, J.D. (1978), A method for estimating foliage-height profiles in broad-leaved forest. *J. Ecol.* 67:35-40.

Aber, J.D. (1979), Foliage-height profiles and succession in Northern Hardwood forest. *Ecology* 60:18-23.

Aber, J.D., Pastor, J.H., and Melillo, J.M. (1982), Changes in forest canopy structure along a site quality gradient in southern Wisconsin. *Am. Midland Naturalist* 108:256-265.

Aldred, A., and Bonner, G. (1985), Application of Airborne Lasers to Forest Surveys, , Petawawa National Forestry Institute, Canadian Forestry Service, Information Report PI-X-51, 61 pp.

Askne, J.I.H., Dammert, P.B.G., Ulander, L.M.H., and Smith, G. (1997), C-Band repeat-pass interferometric SAR observations of the forest. *IEEE Trans. Geosci. Remote Sens.* 35:25-35.

Blair, J.B., Coyle, D.B., Bufton, J.L., and Harding, D.J. (1994), Optimization of an airborne laser altimeter for remote sensing of vegetation and tree canopies. in *Proc. Int.Geosci. Remote Sens. Symp.'94*, California Institute of Technology, Pasadena, CA, pp. 939-941.

Blair, J.B., Rabine, D.L., and Hofton, M.A. (1999), The Laser Vegetation Imaging Sensor (LVIS): A medium-altitude, digitization-only, airborne laser altimeter for mapping vegetation and topography, *ISPRS J. Photogram. Remote Sens.* 54:115-122.

Blair, J.B., and Hofton, M.A. (1999), Modeling laser altimeter return waveforms over complex vegetation using high-resolution elevation data. *Geophys. Res. Lett.,* 26:2509-2512.

Brown, M.J., and Parker, G.G. (1994), Canopy light transmittance in an chronosequence of mixed-species deciduous forests. *Can. J. For. Res.* 24:1694-1703.

Brunig, E.F. (1970), Stand structure, physiognomy and environmental factors in some lowland forests in Sarawak. *Trop. Ecol.* 11:26-43.

Brunig, E.F. (1983), Vegetation structure and growth. in *Tropical Rain Forest Ecosystems - structure and function.* (F.B. Golley, Ed.), Elsevier Scientific Publishing, Amsterdam. pp. 49-75.

Brush, G.S., Lenk, C., and Smith, J. (1980), The natural forest of Maryland: an explanation of the vegetation map of Maryland. *Ecol. Monogr.* 50:77-92.

Bufton, J.L. (1989), Laser altimetry measurements from aircraft and spacecraft, *Proc. IEEE* 77:463-477.

Bufton, J.L., Garvin, J.B., Cavanaugh, J.F., Ramos-Izquierdo, L., Clem, T.D., and Krabill, W.B. (1991), Airborne lidar for profiling of surface topography, *Optical Eng.* 30:72-78.

Chen, J.M., and Cihlar, J. (1996), Retrieving leaf area index of boreal conifer forests using Landsat TM images, *Remote Sens. Environ.* 55:153-162.

Cloude, S.R., and Papathanassiou, K.P. (1998), Polarimetric SAR interferometry. *IEEE Trans. Geosci. Remote Sens.* 36: 1551-1565.

Dammert, P.B.G., and Askne, J. (1998), Interferometric tree height observations in boreal forests with SAR interferometry, in *Proc. Int.Geosci. Remote Sens. Symp.'98*, Seattle, WA, pp.1363-1366.

Demarez, V., Gastellu-Etchegorry, J.P., Mougin, E., Marty, G., Proisy, C., Dufrene, E., and Le Dantec, V. (1999), Seasonal variation of leaf chlorophyll content of a temperate forest. Inversion of the PROSPECT model. *Int. J. Remote Sens.* 20:879-894.

Dobson, M.C., Ulaby, F.T., Pierce, L.E., Sharik, T.L., Bergen, K.M., Kellndorfer, J., Kendra, J.R., Li, E., Lin, Y.C., Nashashibi, A., Sarabandi, K., and Siqueira, P. (1995), Estimation of forest biophysical characteristics in northern Michigan with SIR-C/XSAR. *IEEE Trans. Geosci. Remote Sens.* 33:877-895.

Drake J.B., and Weishampel, J.F. (1998), Multifractal analysis of laser altimeter and ground-based canopy height measures of a longleaf pine savanna. In *Proc. First Int. Conf. Geospatial Infor. Agric. Forestry* , Lake Buena Vista, FL, pp. 403-410.

Dubayah, R., Blair, J.B., Bufton, J.L., Clark, D.B., JaJa, J., Knox, R., Luthcke, S.B., Prince, S., and Weishampel, J. (1997), The Vegetation Canopy Lidar mission, in *Proc. Land Satellite Information in the Next Decade II: Sources and Applications.*, Am. Soc. Photogram. Remote Sens., Bethesda, MD, pp. 100-112.

Ellsworth, D.S. and Reich, P.B. (1993), Canopy structure and vertical patterns of photosynthesis and related leaf traits in a deciduous forest. *Oecologia* 96:169-178.

Eyre. F.H. (editor) (1980), *Forest cover types of the United States and Canada.* Society of American Foresters, Washington, D.C.

Garvin, J., Bufton, J, Blair, J., Harding, D., Luthcke, S., Frawley, J. and Rowlands, D. (1998), Observations of the Earth's topography from the Shuttle Laser Altimeter (SLA): laser-pulse echo-recovery measurements of terrestrial surfaces. *Phys. Chem. Earth.* 23:1053-1068.

Gash, J.H.C. (1979), Analytical model of rainfall interception by forests, *Q. J. Roy. Meteor. Soc.* 105:43-55.

Govaerts, Y. (1995), *A Model of Light Scattering in Three-Simensional Plant Canopies: a Monte Carlo Ray Tracing Approach*, Ph.D. dissertation, Universite Catholique De Louvain, Louvain-la-Neuve.

Hagberg, J.O., Ulander, L.M.H., and Askne, J. (1995), Repeat-pass SAR interferometry over forested terrain. *IEEE Trans. Geosci. Remote Sens.* 33:331-340.

Harding, D.J., Blair, J.B., Garvin, J.B., and Lawrence, W.T. (1994), Laser altimetry waveform measurement of vegetation canopy structure, . in *Proc. Int.Geosci. Remote Sens. Symp.'94*, California Institute of Technology, Pasadena, CA, pp. 1251-1253.

Harding, D.J., Blair, J.B., Rodriguez, E., and Michel, T. (1995), Airborne laser altimetry and interferometric SAR measurements of canopy structure and sub-canopy topography in the Pacific Northwest. in *Proc. Second Topical Symp. Combined Optical - Microwave Earth Atmosphere Sens.* , Atlanta, GA, pp. 22-24.

Harding, D.J. (1998), Airborne lidar observations of canopy structure at the BOREAS tower flux sites. . in *Proc. Int.Geosci. Remote Sens. Symp.'98*, Seattle, WA. pp.1550-1552.

Harding, D.J., Blair, J.B., Rabine, D.L., and Still, K.L. (In Review), Scanning Lidar Imager of Canopies by Echo Recovery (SLICER): Instrument and data product description, *NASA Technical Memorandum.*

Hicks, B.B., Hosker, R.P. Jr., Meyers, T.P., and Womack, J.D. (1991), Dry deposition inferential measurement techniques I. Design and test of a prototype meteorological and chemical system for determining dry deposition, *Atmos. Environ.* 25:2345-3460.

Hofton, M.A., Blair, J.B., Minster, J.-B., Ridgway, J.R., Williams, N.P., Bufton, J.L., and Rabine, D.L. (In Press), An airborne scanning laser altimetry survey of Long Valley, California. *Int. J. Remote Sens.*

Hedman, C.W., and Binkley, D. (1988), Canopy profiles of some Piedmont hardwood forests. *Can. J. For. Res.* 18:1090-1093.

Hollinger, D.Y. (1989), Canopy organization and photosynthetic capacity in a broad-leaved evergreen montane forest. *Funct. Ecol.* 3:53-62.

Horn, H.S. (1971), *The Adaptive Geometry of Trees*, Princeton University Press, Princeton.

Huemmrich, K.F., and Goward, S.N. (1997), Vegetation canopy PAR absorptance and NDVI: an assessment for ten tree species with the SAIL model. *Remote Sens. Environ.* 61:254-269.

Imhoff, M.L. (1995), Radar backscatter and biomass saturation – ramifications for global biomass inventory. *IEEE Trans. Geosci. Remote Sens.* 33:511-518.

Jensen, J.R., Hodgson, M.E., Mackey, H.E. Jr., and Krabill, W. (1987), Correlation between aircraft MSS and LIDAR remotely sensed data on a forested wetland. *Geocarta Int.* 4:39-54.

Jordan, T.E., Correll, D.L., and Weller, D.E. (1993), Nutrient interception by a riparian forest receiving inputs from adjacent cropland. *J. Environ. Qual.* 22:467-473.

Lathrop, R.G., and Pierce, L.L. (1991), Ground-based canopy transmittance and satellite remotely sensed measurements for estimation of coniferous forest canopy structure. *Remote Sens. Environ.* 36:179-188.

Lefsky, M.A. (1997), *Application of Lidar Remote Sensing to the Estimation of Forest Canopy and Stand Structure*, Ph.D. dissertation, University of Virginia, Charlottesville, VA.

Lefsky, M., Cohen, W. Acker, S., Spies, T., Parker, G., and Harding, D. (1998), Lidar remote sensing of forest canopy structure and related biophysical parameters at H.J. Andrews experimental forest, Oregon, USA. . in *Proc. Int.Geosci. Remote Sens. Symp. '98*, Seattle, WA. pp. 1252-1254 pp.

Lefsky, M.J., Harding, D.J., Cohen, W.B., Parker, G.G., and Shugart, H.H. (1999), Lidar remote sensing of forest basal area and biomass: application and theory. *Remote Sens. Environ.* 67:83-98.

Lefsky, M., Cohen, W., Acker, S., Parker, G., Spies, T., and Harding, D. (In Press), Lidar remote sensing of biophysical properties and canopy structure of forests of Douglas-fir and western hemlock. *Remote Sensing Environ.*

Le Toan, T., Beaudoin, A., Riom, J., and Guyon, D. (1992), Relating forest biomass to SAR data. *IEEE Trans. Geosci. Remote Sens.* 30:403-411.

Lowman, M.D. and Wittman, P.K. (1996), Forest canopies: methods, hypotheses, and future directions. *Ann. Rev. Ecol. Syst.* 27: 55-81.

MacArthur, R.H., and Horn, H.S. (1969), Foliage profiles by vertical measurements. *Ecology* 50:802-804.

Maclean, G.A., and Krabill, W.B. (1986), Gross-merchantable timber volume estimation using an airborne LIDAR system. *Canadian Jour. of Remote Sens.* 12:7-18.

Magnussen, S., and Boudewyn, P. (1998), Derivations of stand heights from airborne laser scanner data with canopy-based quantile estimators. *Can. J. For Res.* 28:1016-1031.

Magnussen, S., and Eggermont, P. (In Review), Recovering tree heights from airborne laser scanning data. *Forest Science.*

Means, J.E., Acker, S.A., Harding, D.J., Blair, J.B., Lefsky, M.J., Cohen, W.B., Harmon, M.E., and Mckee, W.A. (1999), Use of large-footprint scanning airborne lidar to estimate forest stand characteristics in the western Cascades of Oregon. *Remote Sens. Environ.* 67:298-308.

Meneti, M., and Ritchie, J.C. (1994), Estimation of effective aerodynamic roughness of Walnut Gulch Watershed with laser altimeter measurements. *Water Resources Re.s.* 30:1329-1337.

Middleton, E.M., Walter-Shea, E.A., Mesarch, M.A., Chan, S.S., and Rusin, R.J. (1998), Optical properties of canopy elements in black spruce, jack pine, and aspen stands in Saskatchewan, *Canada. Can. J. Remote Sens.* 24:169-186.

Monsi, M., and Saeki, T. (1953), Uber den lichtfaktor in den pflanzegeesellschaften und seine bedeutung fur die stoffproduktion. *Jpn. J. Bot.* 14:22-52.

Monsi, M., Uchijima, Z., and Oikawa, T. (1973), Structure of foliage canopies and photosynthesis. *Ann. Rev. Ecol. Syst.* 4:301-327.

Naesset, E. (1997a), Determination of mean tree height of forest stands using airborne laser scanner data. *ISPRS J. Photrogram. Remote Sens.* 52:49-56.

Naesset, E. (1997b), Estimating timber volume of forest stands using airborne laser scanner data, *Remote Sens. Environ.*, 61:246-253.

Nelson, R.F., Krabill, W.B., and Maclean, G.A. (1984), Determining forest canopy characteristics using airborne laser data. *Remote Sens. Environ.* 15:201-212.

Nelson, R., Krabill, W., and Tonelli, J. (1988a), Estimating forest biomass and volume using airborne laser data. *Remote Sens. Environ.* 24:247-267.

Nelson, R., Swift, R., and Krabill, W. (1988b), Using airborne lasers to estimate forest canopy and stand characteristics. *J. Forestry* 86:31-38.

Nelson, R. (1994), *The Use of Airborne Laser Altimetry to Estimate Tropical Forest Basal Area, Volume, and Biomass*, PhD dissertation, Virginia Polytechnic Institute and State University, Blacksburg, VA.

Nelson, R., Oderwald, R., and Gregoire, T.G. (1997), Separating the ground and airborne laser sampling phases to estimate tropical forest basal area, volume, and biomass. *Remote Sens. Eviron.* 60:311-326.

Nemani, R.R., Pierce, L., Running, S., and Band, L. (1993), Forest ecosystem processes at the watershed scale: sensitivity to remotely-sensed leaf area index estimates. *Int. J. Remote Sens.* 14:2519-2534.

Nilsson, M. (1996), Estimation of tree heights and stand volume using an airborne lidar system. *Remote Sens. Environ.* 56:1-7.

Pachepsky, Y.A., Ritchie, J.C., and Gimenez, D. (1997), Fractal modeling of airborne laser altimetry data. *Remote Sens. Environ.* 61:150-161.

Pachepsky, Y.A., and Ritchie, J.C. (1998), Seasonal changes in fractal landscape surface roughness estimated from airborne laser altimetry data. *Int. J. Remote Sens.* 19:2509-2516.

Parker, G.G. (1995), Structure and microclimate of forest canopies. *In Forest Canopies - A Review of Research on a Biological Frontier* (M. Lowman and N. Nadkarni, Eds.). Academic Press, San Diego. pp. 73-106.

Parker, G.G., O'Neill, J.P., and Higman, D. (1989), Vertical profile and canopy organization in a mixed deciduous forest. *Vegetatio.* 85:1-11.

Parker, G.G. and Russ, M.E. (In Review), The canopy surface and stand development: assessing forest canopy structure and complexity with near-surface altimetry. *Ecology.*

Parker, G.G., and Tibbs, D.J. (In Review), Leaf area phenology of a deciduous forest canopy. *J. Ecol.*

Peterjohn, W.T. and Correll, D.L. (1984), Nutrient dynamics in an agricultural watershed: Observations on the role of a riparian forest. *Ecology* 65:1466-1475.

Ranson, K.J., Sun, G. Weishampel, J.F., and Knox, R.G. (1997), Forest biomass from combined ecosystem and radar backscatter modeling. *Remote Sens. Environ.* 59:118-133.

Ritchie, J.C., Everitt, J.H., Escobar, D.E., Jackson, T.J., and Davis, M.R. (1992), Airborne laser measurements of rangeland canopy cover and distribution. *J. Range Management* 45:189-193.

Ritchie, J.C., Humes, K.S., and Weltz, M.A. (1995), Laser altimeter measurements at Walnut Gulch Watershed, Arizona. *J. Soil Water Conser.* 50:440-442.

Ritchie, J.C., Menenti, M., and Weltz, M.A. (1996), Measurements and land surface features using an airborne laser altimeter: The HAPEX-Sahel experiment. *Int. J. Remote Sens.* 17:3705-3724.

Rodriguez, E., Michel, T.R., and Harding, D.J. (In Review), Interferometric measurements of canopy height characteristics for coniferous forests, *Radio Sci.*

Sader, S.A., and Joyce, A.T. (1990), Remote sensing of tropical forests: An overview of research and applications using non-photographic sensors. *Photogr. Eng. Remote Sens.* 56:1343-1351.

Schreier, H., Lougheed, J., Gibson, J.R., and Russell, J. (1984), Calibrating an airborne laser profiling system. *Photo. Eng. Remote Sens.* 50:1591-1598.

Schreier, H. Lougheed, J., Tucker, C., and Leckie, D. (1985), Auto-mated measurements of terrain reflection and height variations using an airborne infrared laser system. *Int. J. Remote Sens.* 6:101-113.

Spanner, M.A., Peterson, D.L. and Running, S.W. (1990), Remote sensing of temperate coniferous forest leaf area index: The influence of canopy closure, understory vegetation and background relectance. *Int. J. Remote Sens.* 11:95-111.

Spies, T.A., and Franklin, J.F. (1991), The structure of natural young, mature, and old-growth Douglas-fir forests in Oregon and Washington. in *USDA Forest Service General Technical Report PNW-GTR.* Pacific Northwest Research Station, Portland, OR, pp. 91-109.

Sun, G., and Ranson, K.J. (1995), A three-dimensional radar backscatter model of forest canopies. *IEEE Trans. Geosci. Remote Sens.* 33:372-382.

Treuhaft, R.N., Madsen, S.E., Moghaddam, M., and Vanzyl, J.J. (1996), Vegetation characteristics and underlying topography from interferometric radar. *Radio Sci.* 31:1449-1485.

Treuhaft, R.N., and Moghaddam, M. (1998), A unified analysis of radar interferometry and polarimetry for the estimation of forest parameters. in *Proc. Int.Geosci. Remote Sens. Symp.'98.*, Seattle, WA, pp. 1373-1375.

Ulaby, F.T., Moore, R.K., and Fung, A.K. (1986), *Microwave Remote Sensing: Active to Passive, Volume III: From Theory to Applications.* Artech House, Norwood, MA.

Vaughn, C.R., Bufton, J.L., Krabill, W.B., and Rabine, D. (1996), Georeferencing of airborne laser altimeter measurements. *Int. J. Remote Sens.* 17:2185-2200.

Weishampel, J.F., Ranson, K.J., and Harding, D.J. (1996), Remote sensing of forest canopies. *Selbyana* 17:6-14.

Weltz, M.A., Ritchie, J.C., and Fox, H.D. (1994), Comparison of laser and field-measurements or vegetation height and canopy cover. *Water Resources Res.* 30:1311-1319.

TABLES

Table 1. SLICER acquisition parameters for the SERC data set.

Laser wavelength	1064 nm (near infrared)
Average ranging distance to ground	5,200 m
Laser beam divergence	~ 2 mrad
Footprint shape	circular
Average footprint diameter (at $1/e^2$)	10.4 m
Footprint spatial energy	radial Gaussian
Cross-track footprints	5
Average cross-track spacing	10.1 m
Average along-track spacing	10.4 m
Vertical sampling	11 cm
Vertical resolution	~ two-thirds of a meter
Height range observed	61 m
Horizontal geolocation accuracy	nominally < 10 m
Vertical geolocation accuracy	nominally < 1 m

Table 2. Summary of stand structure for the four study sites used for SLICER validation.

Characteristic	Site			
	Young	Intermediate	Mature	Old-growth
estimated age (yr)	13	41	99	234
stem density (stems/ha)	5683	840	1187	1373
basal area (m^2/ha)	34.7	39.7	34.7	60.9
highest leaf (m)	17	30	36	41
no. of woody species	9	14	19	22
leaf area index (m^2/m^2)	4.21	5.16	5.26	6.77

Table 3. Maximum and mean heights and height differences for ground observed and averaged SLICER CHPs from the four validation sites.

	CHP Maximum Height				CHP Mean Height			
Site	Ground Observed (m)	SLICER (m)	Ground minus SLICER (m)	Ground minus SLICER (%)	Ground Observed (m)	SLICER (m)	Ground minus SLICER (m)	Ground minus SLICER (%)
Young	17	19	-2	-12	11.5	10.5	1.0	9
Inter-mediate	30	32	-2	-7	15.5	16.4	-0.9	-6
Mature	36	39	-3	-8	18.9	19.8	-0.9	-5
Old-growth	41	45	-4	-10	19.0	21.2	-2.2	-11

Table 4. Results of Chi-square, uneven-sample-size, goodness-of-fit tests (95% confidence) used to determine whether significant differences exist between averaged CHPs for each validation site made with sub-sampled and full SLICER waveforms.

Site	Sub-sampled SLICER Counts	Chi-Square Value	P-Value	Chi-Square Degree of Freedom
Young	578	20.1	0.27	17
Intermediate	974	29.9	0.47	30
Mature	879	47.2	0.12	37
Old-growth	1485	28.1	0.96	44

Table 5. Results of Chi-square, even-sample-size, goodness-of-fit tests (95% confidence) and RMS comparisons of ground CHPs and averaged SLICER CHPs for each validation site.

Site	Chi-Square Value	P-Value	Chi-Square Degree of Freedom	Ground vs. SLICER RMS	Ground vs. Ground RMS
Young	103.6	<0.0001	17	0.014	0.028
Intermediate	215.0	<0.0001	32	0.011	0.020
Mature	164.7	<0.0001	39	0.009	0.014
Old-growth	396.1	<0.0001	43	0.011	0.011

Table 6a. Measurement properties of the ground and SLICER data and resulting effects on the noise level and continuity of the derived CHPs.

Measurement Property	Ground	SLICER	Effect on CHP G = ground S = SLICER
Spatial sampling	uniform point grid	'egg carton' illum-ination	G noisier than S
Distance Accuracy	~ 5% to 10% of observation distance	constant, 11 cm	G noisier than S, esp. high in canopy
Number of total observations	small	very large, oversampled	G noisier than S
No. of observations per CHP bin	fewer at larger distances	fewer at larger distances	G noisier higher S noisier lower
Intrinsic smoothing	none, observations discrete & independent	pulse + detector = sliding window ~ 2/3 m in height	G discrete, stepped S continuous, smoothed

Table 6b. Canopy effects potentially causing elevation biases in ground and SLICER CHPs.

Canopy Property	Ground	SLICER	Effect on CHP G = ground S = SLICER
Non-random horizontal clumping	skewed to shorter distances	Skewed to shorter distances	G biased low S biased high
Leaf angle planophile to eroctophile upward	skewed to shorter distances	Skewed to longer distances	G biased low S biased low
Variability of canopy outer surface height	skewed to shorter distances	Skewed to shorter distances	G biased low S biased low
Canopy vs. ground NIR reflectance ratio (C/G)	not applicable	Actual C/G > 2 : Actual C/G < 2 :	S biased low S biased high
Canopy NIR reflectance increases upward	not applicable	Skewed to shorter distances	S biased high
Multiple scattering	not applicable	Skewed to longer distances	S biased low

Table 7. Ground observed gap fractions (from proportion of clear-sky to total sightings), SLICER gap fractions (from proportion of ground return to total return energy) for canopy to ground reflectance ratios (C/G) equal to one and two, and the C/G required for the SLICER gap fraction to equal the ground observed result.

Site	Ground Observed	SLICER C/G = 1	SLICER C/G = 2	C/G Required for Equal Gap Fractions
Young	0.06	0.044	0.085	1.37
Intermediate	0.05	0.022	0.043	2.34
Mature	0.02	0.023	0.045	0.87
Old-growth	0.06	0.066	0.123	0.91

FIGURE CAPTIONS

Figure 1. Illustration of backscatter return energy as a function of travel time (gray shaded distribution) for a single laser pulse, with the start, peak and end of the ground return indicated. Travel time is converted to distance based on the speed of light through a standard atmosphere, yielding canopy height from the distance between the highest detected canopy top (time interval unit (TIU) stop) and ground return start. The cumulative distribution of return energy (solid curve), accumulated downward from the canopy top and normalized, is a measure of canopy closure (not corrected for differences in reflectance of the ground and canopy).

Figure 2. Perspective views of laser pulse Gaussian energy distribution for a single SLICER footprint (left) and a 5 x 5 array of footprints (right). The average footprint diameter in this study, defined where the energy decreases to $1/e^2$ (i.e., 13.5%) of the peak (gray circle, left), is 10.4 m based on a 2 mrad divergence of the transmitted laser pulse and the average ranging distance to the ground. The 5 x 5 array is composed of footprints with cross-track and along-track spacing equal to the footprint diameter. In this ideal case, the energy minima between footprints decrease to 8% of the peaks.

Figure 3. Map of SLICER ground tracks (solid lines) and study sites (triangle: young stand; square: intermediate-age and mature stands within SERC stem map; diamond: old-growth stand) southwest of Annapolis on the western shore of Chesapeake Bay.

Figure 4. Sampling geometry for the intermediate-age stand within the SERC stem map depicting the SLICER swath, composed of 5 cross-track footprints (open circles), and ground sampling grid (filled circles). The position of the SLICER footprints as shown

with respect to the ground grid is illustrative; the relative position accuracy between the two data sets is approximately 10 m due to geolocation uncertainty.

Figure 5. Transformation steps converting a raw SLICER waveform to a canopy height profile: a) raw waveform with 0.11 m sampling interval for a single laser pulse, b) waveform above mean background noise summed to 0.66 m sampling interval, and start, peak, and end of the ground return identified, c) cumulative distributions of canopy closure (solid), assuming ground reflectance that is half that of the canopy, and transformation to projected plant area (dashed) applying the MacArthur-Horn methodology, and d) normalized, incremental distribution of plant area above ground.

Figure 6. Ground track map for the SLICER flight lines (numbered 1 to 6) across the SERC stem map comprised of intermediate-age (cross-hatched) and mature (diagonal pattern) stands, with the ground sampling plots outlined (I and M, respectively) and the location of the SLICER footprint on the flux tower indicated by the filled circle (T).

Figure 7. SLICER average canopy height profiles per flight line (solid, shaded, and dashed distributions) from the areas of overlap at the ground track intersections within the SERC stem map.

Figure 8. SLICER canopy height profile transects across: a) the young stand study site and adjacent stands, b) the intermediate-age and mature stands within the SERC stem map (flight line 3), and c) the old-growth stand, with ground sampling plot (gsp) locations indicated. Canopy height profiles are computed for individual laser shots along a single, cross-track footprint position within the SLICER swath. Darker gray shading corresponds to a greater fraction of plant area within a footprint. The width of the gray-scale columns corresponds to the diameter of each laser footprint. The solid, bold line and thin ticks

indicate the elevation of the start of the ground return and the canopy top, respectively. Elevations are referenced to the WGS-84 ellipsoid which is 33 m above mean sea level in the study region. Vertical exaggeration is 5:1.

Figure 9. Height distributions for un-transformed observations (left panel), incremental canopy height profiles (center panel), and cumulative canopy height profiles (right panel) for the four study sites. SLICER results are shown as solid lines. Ground results are shown as dashed lines in the left and right panels, and as distribution bins in the center panel. Un-transformed observations for the ground are the intercept sightings and for SLICER are the summed, above-ground waveform amplitudes, with each normalized. All results are binned at 1 m.

Figure 10. Effect of ground return scale factor on SLICER canopy height profiles. Solid, shaded, and dashed distributions correspond to scale factors of 1, 2, and 4, respectively (equivalent to an average ground reflectance at 1064 nm and 0° phase angle equal to, one-half, and one-quarter that of the canopy).

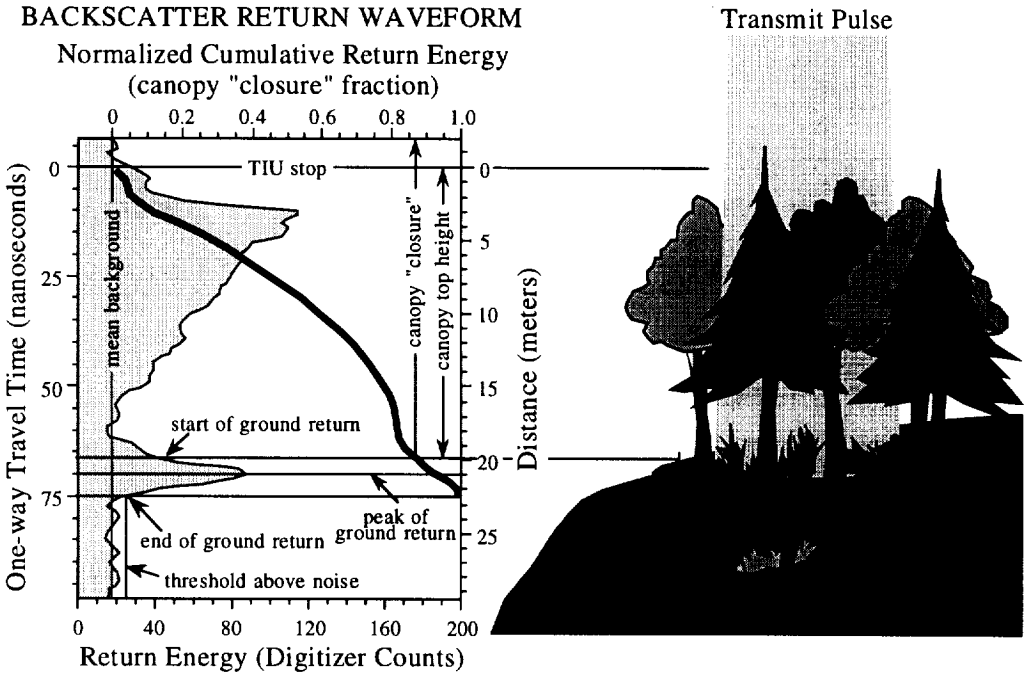
BACKSCATTER RETURN WAVEFORM
Normalized Cumulative Return Energy
(canopy "closure" fraction)
0
0.2
0.4
0.6
0.8
1.0
TIU stop
mean background
canopy "closure"
canopy top height
start of ground return
peak of ground return
end of ground return
threshold above noise
One-way Travel Time (nanoseconds)
0
25
50
75
Distance (meters)
0
5
10
15
20
25
0
40
80
120
160
200
Return Energy (Digitizer Counts)
Transmit Pulse

Figure 1.

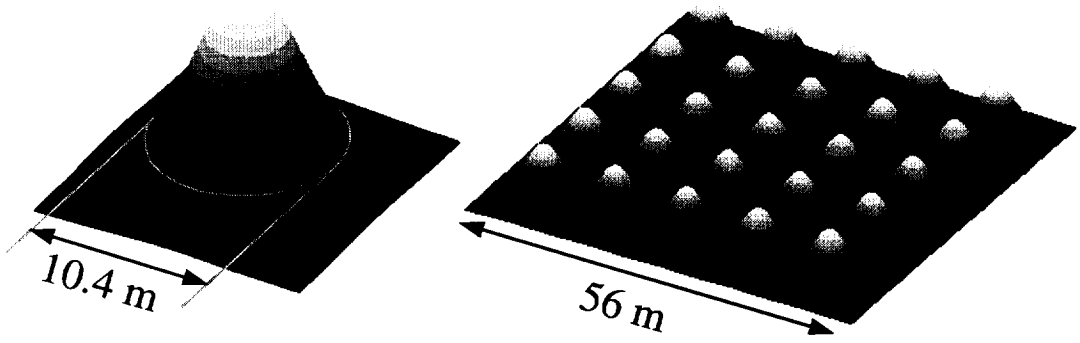

Figure 2.

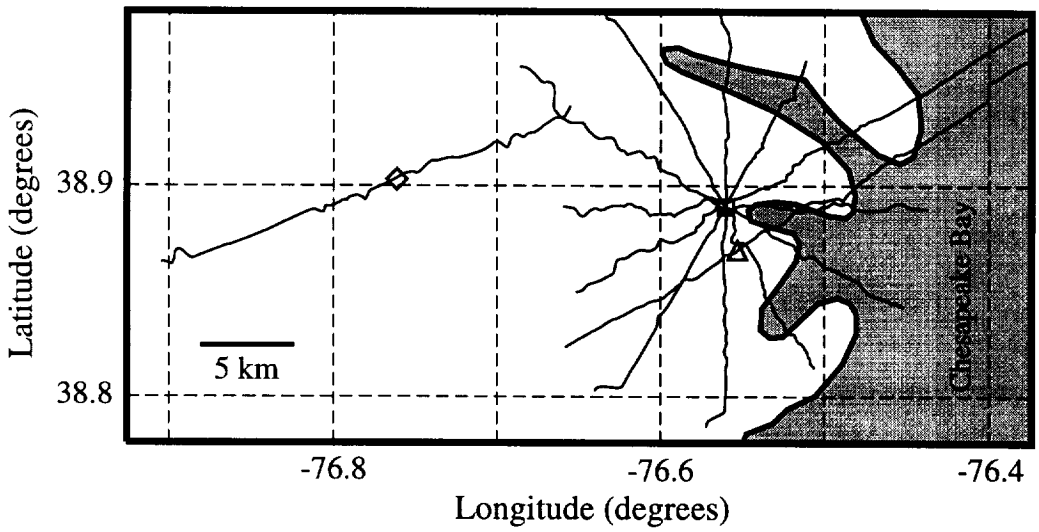
Latitude (degrees)
38.9
38.8
5 km
Chesapeake Bay
-76.8
-76.6
-76.4
Longitude (degrees)

Figure 3.

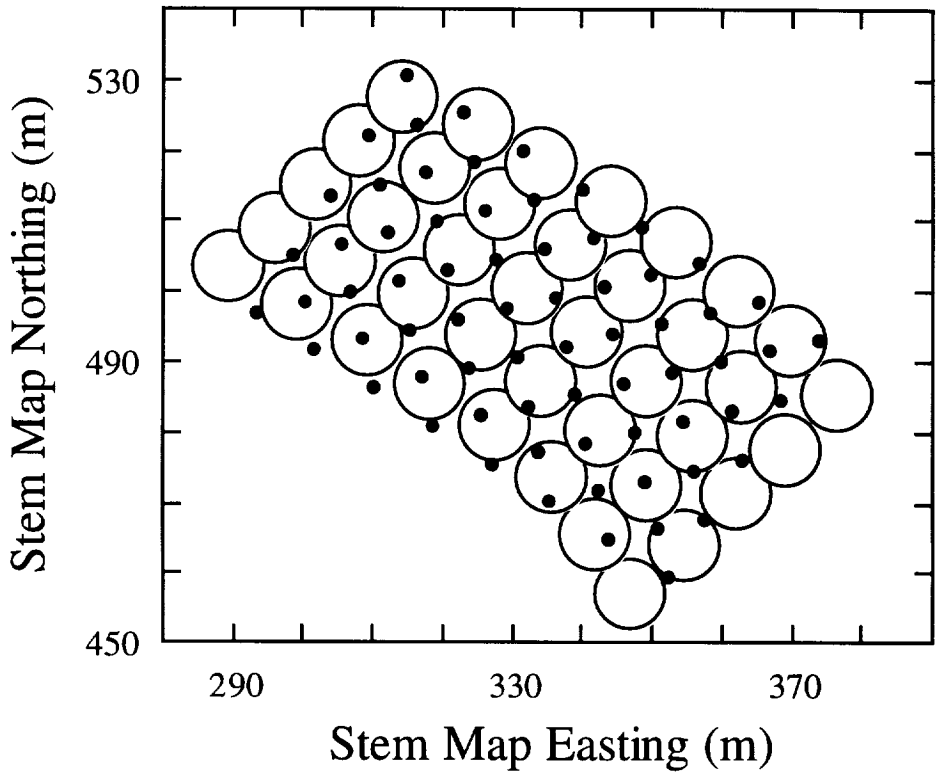

Figure 4.

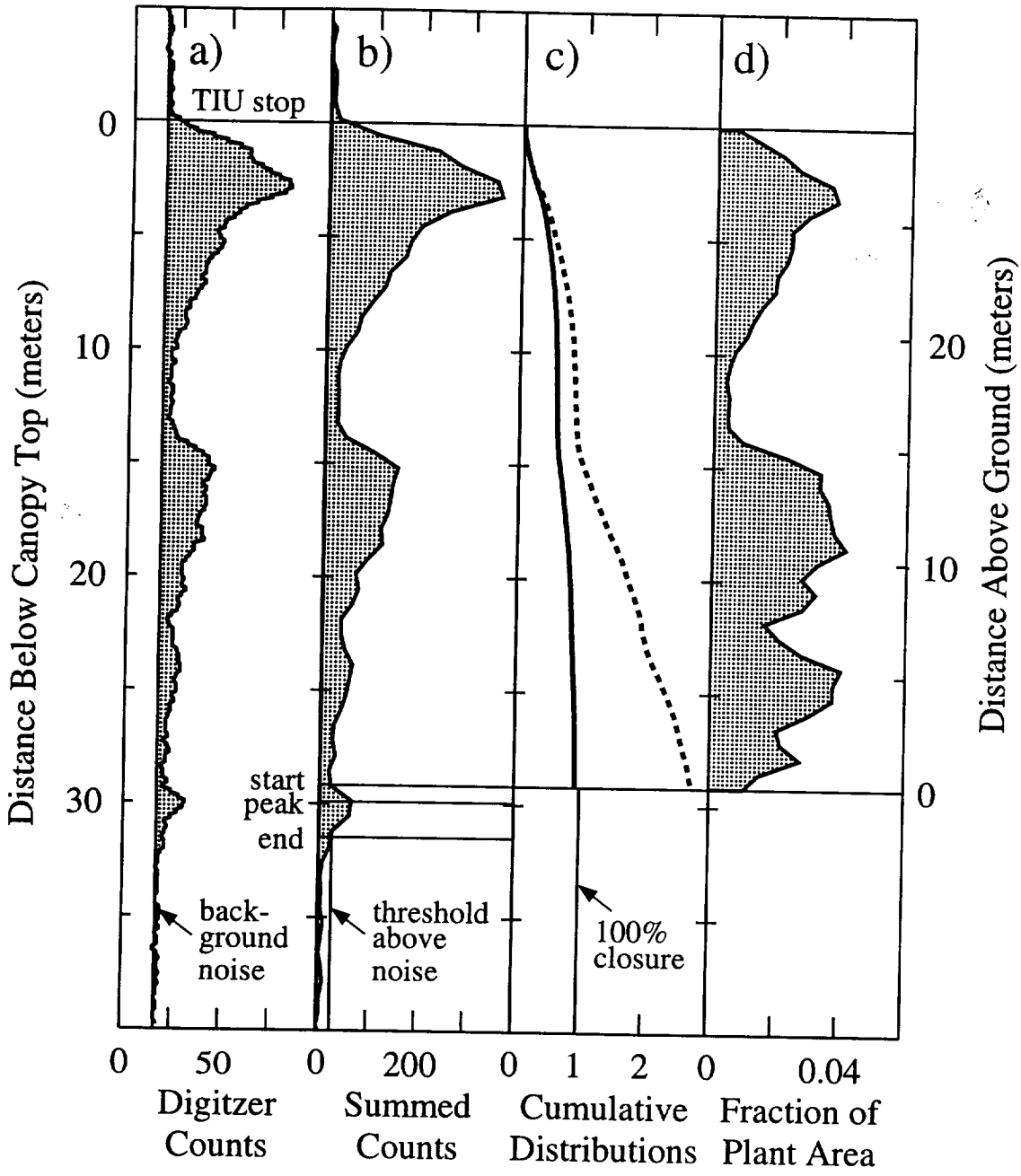
a)
b)
c)
d)
TIU stop
0
10
20
30
start
peak
end
back-
ground
noise
threshold
above
noise
100%
closure
Distance Below Canopy Top (meters)
Distance Above Ground (meters)
0
10
20
0
0
50
0
200
0
1
2
0
0.04
Digitzer
Counts
Summed
Counts
Cumulative
Distributions
Fraction of
Plant Area

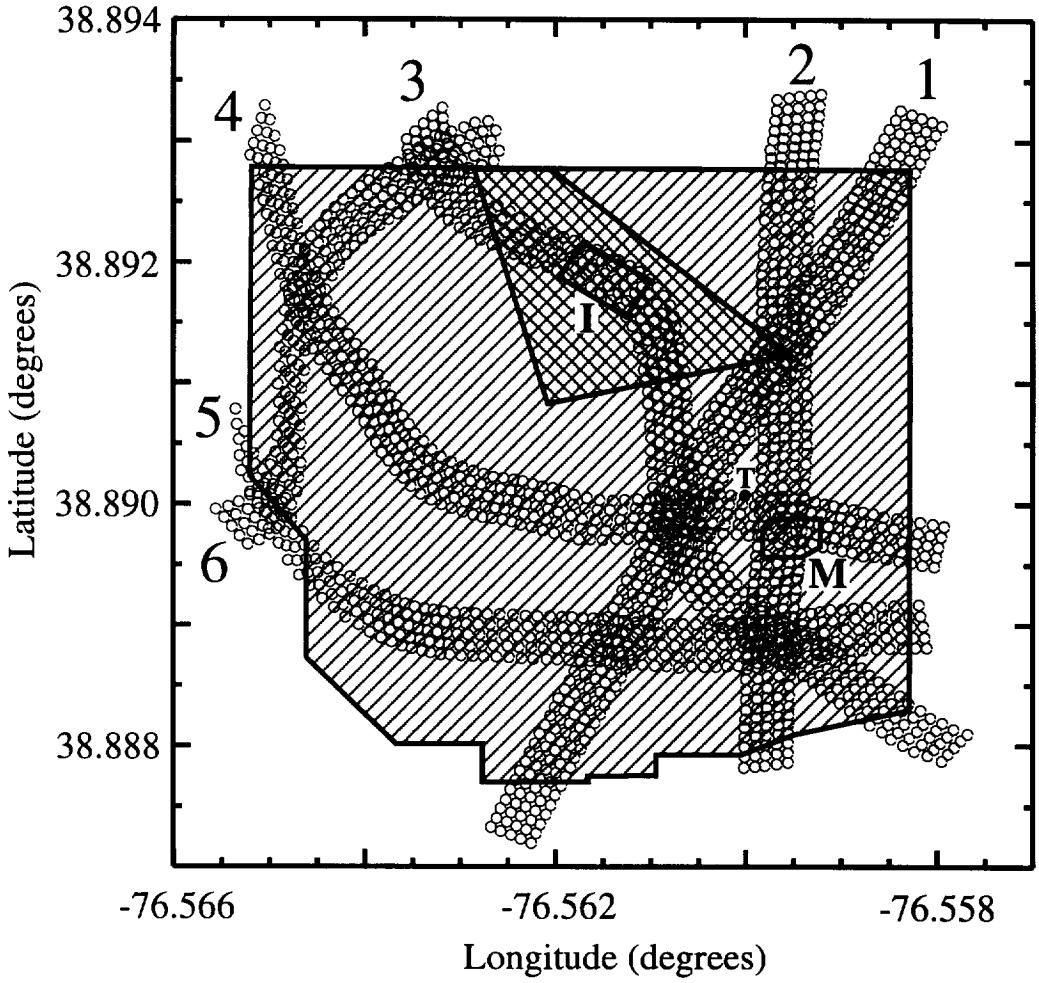
38.894
38.892
38.890
38.888
Latitude (degrees)
-76.566
-76.562
-76.558
Longitude (degrees)
1
2
3
4
5
6
I
T
M

Figure 6.

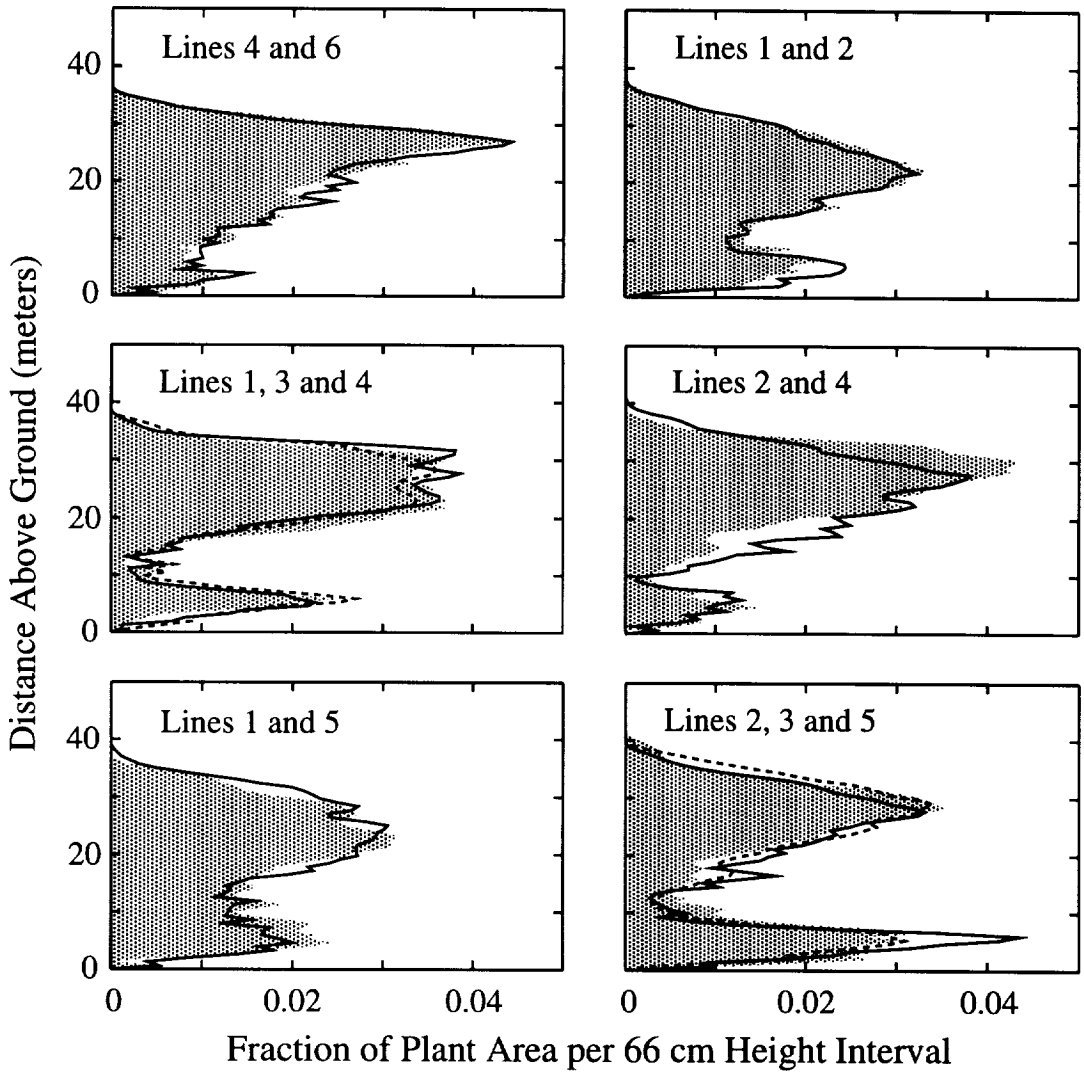
Lines 4 and 6
Lines 1 and 2
Lines 1, 3 and 4
Lines 2 and 4
Lines 1 and 5
Lines 2, 3 and 5
40
20
0
0
0.02
0.04
Distance Above Ground (meters)
Fraction of Plant Area per 66 cm Height Interval

Figure 7.

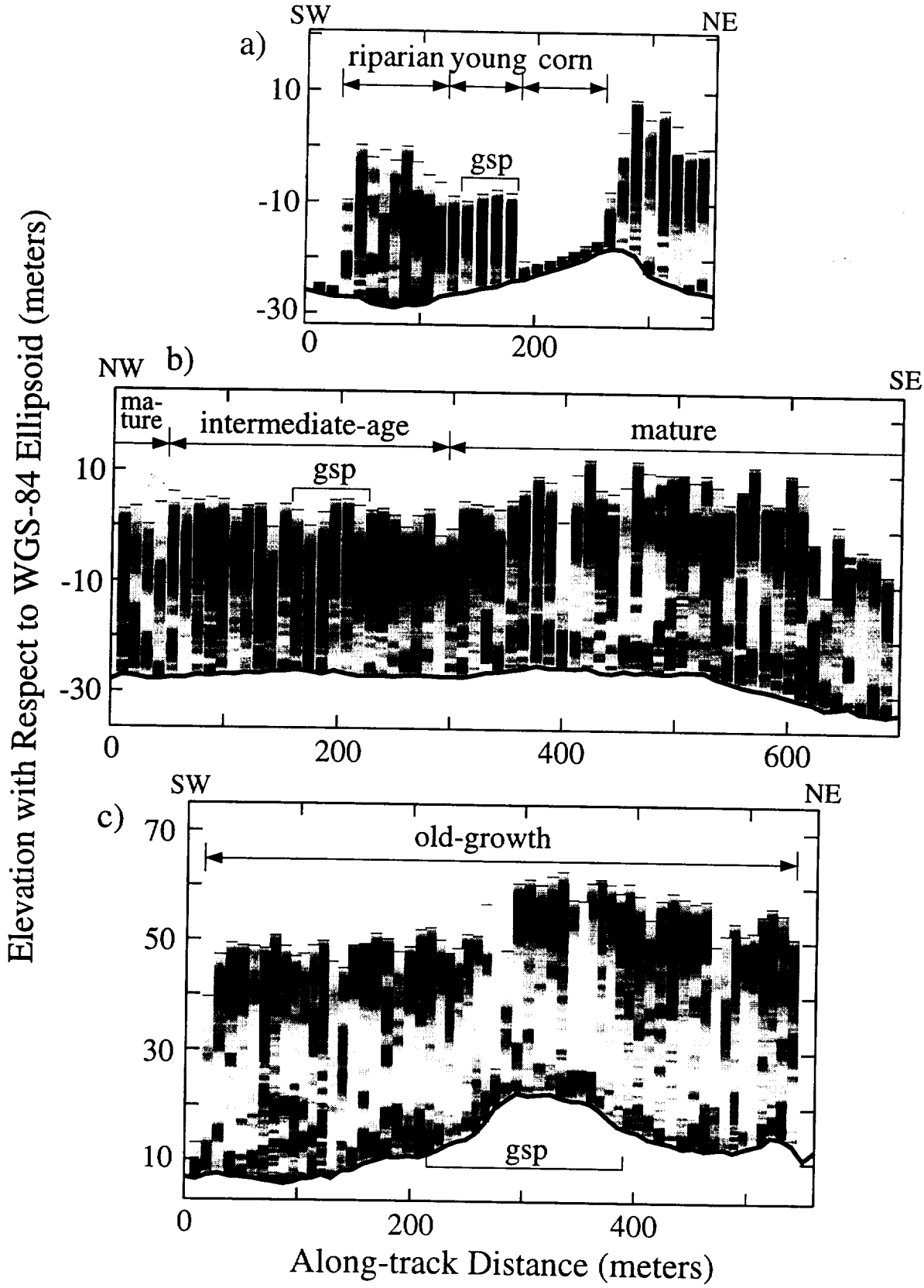
a)
SW
NE
riparian
young corn
gsp
10
-10
-30
0
200
b)
NW
SE
ma-
ture
intermediate-age
mature
gsp
10
-10
-30
0
200
400
600
c)
SW
NE
old-growth
70
50
30
10
gsp
0
200
400
Elevation with Respect to WGS-84 Ellipsoid (meters)
Along-track Distance (meters)

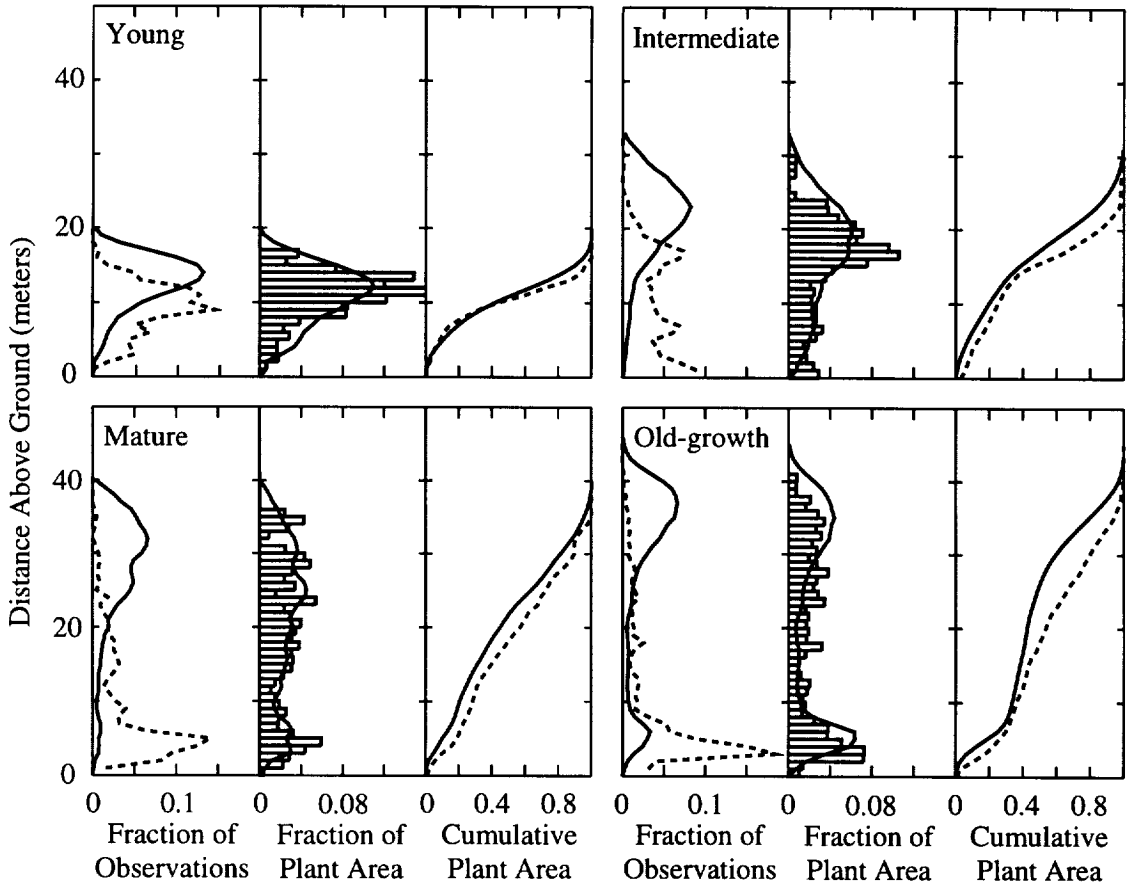
Young
Intermediate
Mature
Old-growth
Distance Above Ground (meters)
0
20
40
0
0.1
0.08
0.4
0.8
Fraction of Observations
Fraction of Plant Area
Cumulative Plant Area

Figure 9.

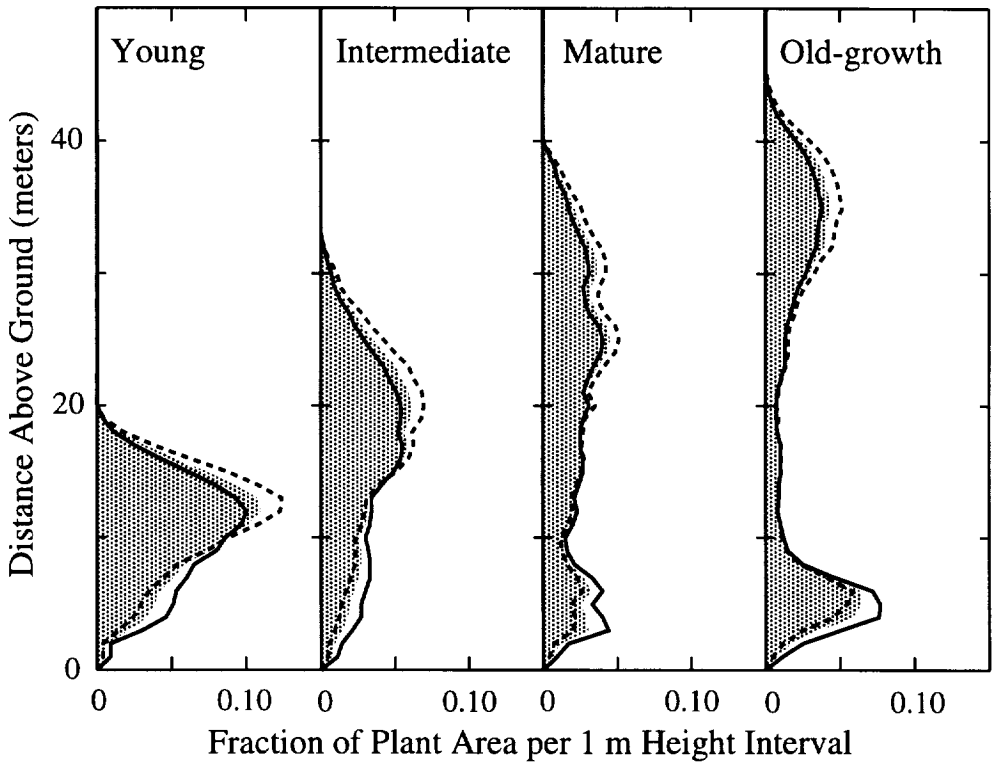
Young
Intermediate
Mature
Old-growth
Distance Above Ground (meters)
40
20
0
0
0.10
0
0.10
0
0.10
0
0.10
Fraction of Plant Area per 1 m Height Interval

Figure 10.